

SCALE INVARIANT THEORY OF FULLY DEVELOPED HYDRODYNAMIC TURBULENCE— HAMILTONIAN APPROACH

V.S. L'VOV*

Meyerhoff Visiting Professor, Department of Nuclear Physics, The Weizmann Institute of Science, 76100 Rehovot, Israel

Editor: I. Procaccia

Received February 1991

Contents:

Historical introduction	3	8. Asymptotic behavior of the Green function G and the pair correlation function N in s and ω	24
1.1. Equations of motion	3	8.1. Asymptotic behavior of the functions $G(r - r_0, k, \omega)$ and $N(r - r_0, k, \omega)$ in the mixed r, k representation	24
1.2. Transition to turbulence	4	8.2. Asymptotic behavior of the functions $G(k + s/2, k - s/2, \omega)$ and $N(k + s/2, k - s/2, \omega)$ in the s, k representation	26
1.3. Richardson—Kolmogorov—Obukhov picture of turbulence	4	9. Kolmogorov—Obukhov scaling and the asymptotic form of multipoint correlation functions	28
1.4. Intermittency	6	9.1. Scaling relation	28
1.5. Analytic approach to turbulence studies	7	9.2. Dynamic relation for the scaling indices	28
<i>Part I. Physical introduction to the theory, results and discussion</i>	10	9.3. Multipoint one-time velocity correlation functions	31
1. The problem of eliminating the sweeping interaction in the theory of turbulence	10	<i>Part II. Mathematical apparatus of the theory</i>	32
1.1. Dynamic and sweeping interactions	10	10. Diagram technique for the quasi-Lagrangian Clebsch variables b and b^*	32
1.2. Sweeping interaction and infrared divergences	11	11. Analysis of diagram convergence in the quasi-classical approximation	34
1.3. In which region is it really necessary to eliminate sweeping?	12	11.1. The Dyson—Wyld equations in the quasi-classical approximation	34
2. Quasi-Lagrangian method of local elimination of the sweeping interaction	13	11.2. Reduction of the diagram technique to three-dimensional form	34
3. Local statistical characteristics $G(r, k, \omega)$ and $F(r, k, \omega)$ of the turbulent velocity field	14	11.3. Analysis of the IR convergence of three-dimensional diagrams	35
4. Scale invariant limit in the theory of fully developed turbulence	16	11.4. Analysis of the UV convergence of three-dimensional diagrams	37
5. Hamiltonian approach to the theory of turbulence of an incompressible fluid	16	12. Structural functions of the quasi-Lagrangian theory and locality of the interaction	38
5.1. Canonical equations of motion	16	12.1. Reduction of the canonical quasi-Lagrangian diagram technique to three-dimensional form	38
5.2. Are the Hamiltonian and traditional approaches to the theory of turbulence equivalent?	17	12.2. Asymptotic behavior of the Green function G and the pair correlation function N for $s \gg k$	39
6. Formulation of the Hamiltonian theory of the dynamic interaction of eddies	18	12.3. Asymptotic behavior of the functions G and N for $L^{-1} \ll s \ll k$	39
6.1. Elimination of the sweeping interaction	18	13. Direct calculation of the Green function and the pair correlation function diagonal in s	41
6.2. Derivation of the equations of motion for b and b^*	19	14. Calculation of the asymptotic behavior of the structural functions for large frequencies	44
6.3. On the diagrammatic perturbation theory for b and b^*	20	15. Conclusion	45
6.4. What is the consequence of the nondiagonality of the theory in the momenta?	21	References	46
7. A scheme to prove the hypothesis of locality of the dynamic interaction of eddies	22		
7.1. Quasi-classical approximation	22		
7.2. How to prove the IR and UV convergence of all integrals in diagrams of any order at least in the quasi-classical approximation	23		
7.3. A scheme to prove convergence of integrals in the quasi-Lagrangian nondiagonal diagram technique	24		

* Permanent address: Institute of Automation and Electrometry, Siberian Division of the USSR Academy of Sciences, 630090 Novosibirsk, USSR.

**SCALE INVARIANT THEORY
OF FULLY DEVELOPED
HYDRODYNAMIC TURBULENCE—
HAMILTONIAN APPROACH**

V.S. L'VOV

*Meyerhoff Visiting Professor, Department of Nuclear Physics,
The Weizmann Institute of Science, 76100 Rehovot, Israel*



NORTH-HOLLAND

Abstract:

The statistical theory of fully developed homogeneous turbulence of an incompressible fluid presented here is based on the Hamiltonian equations for an ideal fluid in the Clebsch variables using the Wyld diagram technique. This theory is formulated in terms of the local Green function $G(\mathbf{r}, \mathbf{k}, \omega)$ and the local pair correlation function $N(\mathbf{r}, \mathbf{k}, \omega)$ describing the statistical properties of k -eddies in the vicinity of point \mathbf{r} .

One of the major difficulties arising from the masking effect of the sweeping interaction is effectively solved by transforming to a moving reference system associated with the fluid velocity in some reference point \mathbf{r}_0 . This change of coordinates eliminates the sweeping of k -eddies in a region of scale $1/k$ surrounding the reference point \mathbf{r}_0 . The convergence of all the integrals in the diagrams of arbitrary order of perturbation theory both in the IR and UV regions, is proved. This gives a diagrammatic proof of the Kolmogorov–Obukhov hypothesis that the dynamic interaction of eddies is local.

In the inertial interval, the scale invariant solution of the Dyson–Wyld diagram equations has been obtained, which is consistent with the known Richardson–Kolmogorov–Obukhov concept of fully developed uniform turbulence. This new theory provides techniques for calculating the statistical characteristics of turbulence. For the purpose of illustration the asymptotic form of the simultaneous many-point velocity correlation functions when one of the wave vectors or the sum of a group of wave vectors tends to zero, is calculated.

Though there is not yet a consistent theory of turbulence, we believe, that the correct way of its development has been found.

L.D. Landau and E.M. Lifshitz, *Fluid Mechanics* [1]

Historical introduction*1.1. Equations of motion*

The word *turbulence* is used to describe diverse phenomena. Among these phenomena *hydrodynamic turbulence* is one of the important, hard to describe, interesting and challenging problems. Hydrodynamic turbulence occurs in a very wide variety of liquid and gas flows ranging from the mixing of a cocktail to the behavior of the atmosphere, from the blood flow in a vessel to the flow in tubes, rivers, seas and the ocean, from thermal convection in a saucepan when soup is prepared to thermal convection in stars, from air flows around pedestrians, automobiles and aircraft to liquid and gas flows in technical devices.

Physical hydrodynamics as a science was founded by L. Euler, C. Navier and G. Stokes. In 1755 Leonard Euler suggested the equation of motion of an ideal fluid, later named the Euler equation,

$$\frac{\partial \mathbf{v}(\mathbf{r}, t)}{\partial t} + [\mathbf{v}(\mathbf{r}, t) \cdot \nabla] \mathbf{v}(\mathbf{r}, t) + \frac{\nabla p(\mathbf{r}, t)}{\rho(\mathbf{r}, t)} = 0. \quad (\text{I.1})$$

$\mathbf{v}(\mathbf{r}, t)$ is the velocity field, $p(\mathbf{r}, t)$ is the pressure and $\rho(\mathbf{r}, t)$ is the density of the liquid or gas. Sometime later, in 1827, G. Navier took into account the viscosity with the help of model considerations,

$$\frac{\partial \mathbf{v}(\mathbf{r}, t)}{\partial t} + [\mathbf{v}(\mathbf{r}, t) \cdot \nabla] \mathbf{v}(\mathbf{r}, t) + \frac{\nabla p(\mathbf{r}, t)}{\rho(\mathbf{r}, t)} = \nu \Delta \mathbf{v}(\mathbf{r}, t). \quad (\text{I.2})$$

ν is the kinematic viscosity (usual viscosity divided by density). In 1845 G. Stokes gave a modern derivation of the Navier–Stokes (NS) equation (I.2).

The next important step in the development of hydrodynamics was made by Honore Reynolds. In 1883 he experimentally proved that the character of the flow of a fluid does not depend on its velocity and viscosity separately. Under certain boundary and initial conditions, the character of the flow depends on the dimensionless ratio $\text{Re} = [\text{nonlinear term in NS equation}]/[\text{viscosity term in NS}]$

equation], which is the Reynolds number,

$$\text{Re} = \frac{(\mathbf{v} \cdot \nabla) \mathbf{v}}{\nu \Delta \mathbf{v}} \approx \frac{v^2/L}{\nu v/L^2} = \frac{vL}{\nu}. \quad (\text{I.3})$$

Here L is the characteristic scale of the velocity field $\mathbf{v}(\mathbf{r}, t)$. It is interesting to estimate Re for some typical problems, for example, for water flow in a river. Put $v \approx 100$ cm/s, depth $L \approx 10^3$ cm, $\nu = 0.01$ cm²/s (for water); then $\text{Re} \approx 10^7$. For a typical atmospheric flow one can put $v \approx 10^3$ cm/s, $L \approx 10^3$ – 10^4 cm, $\nu \approx 0.15$ (for air) and obtain $\text{Re} \approx 5 \times (10^4$ – $10^5)$.

1.2. Transition to turbulence

What is the difference between liquid flow in the limits $\text{Re} \ll 1$ and $\text{Re} \gg 1$? For $\text{Re} \ll 1$, the nonlinear term in the NS equation (I.2) is negligible and the flow is *laminar* in the sense that it will display regular and predictable variations in both space and time. For $\text{Re} \gg 1$ the NS equation (I.2) is essentially nonlinear, which makes its study extremely difficult. In this case experimentally the fluid behavior turns out to be complex, unpredictable, chaotic, i.e. *turbulent*.

The question is: what is the origin of the laminar–turbulent transition? The complete answer is difficult and lies beyond the framework of this paper, but the first step is easy: at some $\text{Re} = \text{Re}_{\text{cr}}$ (usually Re_{cr} lies in the range between unity and a hundred) a laminar flow loses its stability and a secondary flow arises. The classical examples of secondary flows are the following: Taylor vortices in the circular Couette flow (between two rotating coaxial cylinders), Bénard cells in a fluid layer heated from below and so on. As the Reynolds number increases further, secondary flows typically undergo a sequence of instabilities until, in the limit of $\text{Re} \rightarrow \infty$, they become *fully turbulent*.

1.3. Richardson–Kolmogorov–Obukhov picture of turbulence

The modern concept of fully developed hydrodynamic turbulence is based on Richardson's cascade model (1922) [1–3]: for $\text{Re} = vL/\nu \gg 1$ (v is the velocity of flow, L is the size of a streamlined body) the initial flow is unstable. The development of this instability leads to eddies with size $L_1 < L$ and velocity $v_1 < v$. Therefore the Reynolds number $\text{Re}_1 = v_1 L_1 / \nu$ calculated with the quantities v_1 and L_1 is somewhat smaller than $\text{Re} = vL/\nu$. But $\text{Re}_1 \gg 1$ and these eddies are unstable too. So they decay into secondary eddies with size L_2 and velocity v_2 smaller than L_1 and v_1 . Then $\text{Re}_2 = v_2 L_2 / \nu < \text{Re}_1$ but $\text{Re}_2 \gg 1$ and secondary eddies are unstable as well. These eddies in their turn decay into third-generation vortices, which also decay and so on and so-forth. This cascade of decays goes on until the Reynolds number calculated with the help of the size and velocity of n th generation eddies is about some Re_{cr} ,

$$\text{Re} > \text{Re}_1 > \text{Re}_2 > \dots > \text{Re}_n \approx \text{Re}_{\text{cr}}. \quad (\text{I.4})$$

The last-generation eddies are stable and they dissipate due to viscosity. The description of fully developed turbulence must be statistical.

One of the aims of the theory is the calculation of the correlation functions of the velocity field $\mathbf{v}(\mathbf{r}, t)$ which define the statistical properties of turbulence. Of most importance is the pair correlation function $F(\mathbf{k})$, characterizing the energy distribution of turbulence $E(k)$ in different scales. For stationary

uniform isotropic turbulence of an incompressible fluid [2]

$$F_{ij}(\mathbf{k})\delta(\mathbf{k} - \mathbf{k}_1) = \langle v_i(\mathbf{k}, t) v_j^*(\mathbf{k}_1, t) \rangle, \quad (\text{I.5})$$

$$F_{ij}(\mathbf{k}) = P_{ij}(\mathbf{k})F(k), \quad P_{ij}(\mathbf{k}) = \delta_{ij} - k_i k_j / k^2, \quad (\text{I.6})$$

$$E(k) = 2\pi\rho k^2 F(k). \quad (\text{I.7})$$

Here \mathbf{k} is the wave vector or momentum, $\mathbf{v}(\mathbf{k}, t)$ is the Fourier transform of $\mathbf{v}(\mathbf{r}, t)$ (or the velocity field in \mathbf{k}, t representation), $P_{ij}(\mathbf{k})$ is the transverse projection operator and ρ is the density of the fluid.

An important contribution to the theory of fully developed turbulence was made by Kolmogorov and Obukhov in 1941 [4, 5]. They assumed that in the cascade the process of energy transfer between eddies of different scales is local and all detailed statistical information on the source of energy in the large scales L is lost except the injection rate ε , because it equals the energy flux (and also the dissipation rate). Since the dissipation is negligible at scales $r \gg L_n$, the viscosity does not enter the energy spectrum $E(k)$. Therefore, the form of the spectrum $E(k)$ is independent of both L_1 and L_n in the inertial interval

$$L_1 \gg r \gg L_n, \quad (\text{I.8})$$

and $E(k)$ is defined only by the density ρ , momentum k and energy flux through the scale ε , and dimensional analysis yields

$$E(k) = c_{\text{KO}}(\varepsilon/\rho)^{2/3} k^{-5/3}. \quad (\text{I.9})$$

Note that independently but later the scaling law (I.9) was discovered by Onsager (1945) [6], Heisenberg (1948) [7] and von Weizsäcker (1948) [8]. Using the quantities ε , ρ and $k = 2\pi/r$ it is possible to estimate also:

– the rotation velocity of r -eddies (turbulent fluid motion with the characteristic spatial scale r),

$$v(r) \simeq (\varepsilon r/\rho)^{1/3}, \quad (\text{I.10a})$$

– the vorticity $\boldsymbol{\omega} = \text{rot } \mathbf{v}$ of r -eddies,

$$\omega(r) \simeq (\varepsilon/\rho)^{1/3} r^{-2/3}, \quad (\text{I.10b})$$

which tends to infinity as $r \rightarrow 0$,

– the rotation frequency

$$\gamma(r) \simeq v(r)/r \simeq (\varepsilon/\rho)^{1/3} r^{-2/3} \simeq (\varepsilon/\rho) k^{2/3}, \quad (\text{I.10c})$$

– the lifetime of r -eddies,

$$\tau(r) \simeq (\rho/\varepsilon)^{1/3} r^{2/3}. \quad (\text{I.10d})$$

Obviously, $\gamma(r)\tau(r) \approx 1$, because there are no dimensionless parameters in the KO theory for the inertial region. Using eq. (I.10a) one can estimate the *current Reynolds number* for r -eddies,

$$\text{Re}(r) = v(r)r/\nu \approx (\varepsilon/\rho)^{1/3} r^{4/3}, \quad (\text{I.11})$$

and then from the condition $\text{Re}(r) \approx \text{Re}_{\text{cr}}$ estimate the characteristic size of last-generation eddies in the cascade of decays, which are stable and dissipate due to viscosity,

$$L_n \approx \text{Re}_{\text{cr}}^{3/4} (\rho/\varepsilon)^{1/4}. \quad (\text{I.12a})$$

The scale L_n is usually called the *internal, dissipative* or *viscosity scale of turbulence* and designated as L_{int} or L_{dis} ($L_{\text{int}} \equiv L_{\text{dis}} \equiv L_n$). The size of the largest eddies L_1 is usually called the *external* or *energy-contained scale of turbulence*: $L_{\text{ext}} \equiv L_1$. It is useful to express L_{ext} via the external Reynolds number $\text{Re} = v(L_{\text{ext}})L_{\text{ext}}/\nu$ and the quantities ε and ρ [see eq. (I.10a)],

$$L_{\text{ext}} = \text{Re}^{3/4} (\rho/\varepsilon)^{1/4}. \quad (\text{I.12b})$$

Equations (I.12a) and (I.12b) together yield

$$L_{\text{int}} \approx L_{\text{ext}} (\text{Re}_{\text{cr}}/\text{Re})^{3/4}. \quad (\text{I.12c})$$

In such a way we obtain the well-known estimate for the Re dependence of the number of dynamically active degrees of freedom in a volume of turbulence L_{ext}^3 [1, 2],

$$N(\text{Re}) \approx L_{\text{ext}}^3/L_{\text{int}}^3 \approx (\text{Re}/\text{Re}_{\text{cr}})^{9/4}. \quad (\text{I.13})$$

For modest geophysical standards one can put $\text{Re} \approx 10^7$ – 10^8 , $\text{Re}_{\text{cr}} \approx 10$ and obtain $N \approx 10^{14}$ – 10^{16} (!!!).

I.4. Intermittency

In the 40s Landau [1] indicated that the Kolmogorov–Obukhov law (I.9) and the other results (I.10–I.13) based on the dimensionality consideration were not so obvious as it seemed as first glance. Indeed, the property of intermittency is inherent in turbulence, i.e., all the quantities that characterize it suffer from strong fluctuations. So, the turbulence spectrum $E(k)$ can be described by an average energy flow and also dispersion, which in the case of strong fluctuations may depend on the parameter kL characterizing the number of successive crushings of k -eddies required for reducing its size from L to k^{-1} . Experimental evidence of intermittency of flows was given by Batchelor and Townsend in 1949 [10] and then Kuo and Corrsin in 1971, 1972 [11, 12].

Kolmogorov (1962) [13], Obukhov (1962) [14] and after them Novikov and Stewart (1964) [15], Yaglom (1966) [16], Mandelbrot (1974, 1976) [17, 18], Frisch, Sulem and Nelkin (1978) [19] have proposed modifications of the KO theory to take intermittency into account. The energy cascade is described as a breakdown process of eddies into smaller eddies which fill a lesser portion of space with a spatial distribution prescribed by the model. The statistics of the velocity field at scale $1/k$ then depends upon the number of steps required to generate eddies of size $1/k$ starting from eddies of size L_1 . As a result the dimensionless parameter kL_{ext} enters the expression for $E(k)$, to an unknown though not very

large degree [2],

$$E(k) \sim (\varepsilon/\rho)^{2/3} k^{-5/3} (kL_{\text{ext}})^{-\rho}. \quad (\text{I.14})$$

Remaining on the phenomenological level of the argument we present some considerations in favor of the fact that the turbulence spectrum may also depend on the internal scale L_{int} ,

$$E(k) \sim (\varepsilon/\rho)^{2/3} k^{-5/3} (kL_{\text{ext}})^{-\rho} (kL_{\text{int}})^{\mu}. \quad (\text{I.15})$$

Indeed, the interaction of eddies of scale k , defining the spectral energy flow, may be dependent on how strongly they are cut by the eddies of the internal scale, which thus can serve as ‘‘catalysts’’ for the interaction process. The probability still exists that the form of the spectrum $E(k)$ is influenced by a rather weak process of energy exchange between the vortices of the scales L_{int} and $1/k$. Therefore the form of the spectrum cannot be determined by a phenomenological approach to the description of developed turbulence. Because of this, many attempts have been undertaken to construct a theory in a microscopic way directly from the Navier–Stokes equation (I.2).

1.5. Analytic approach to turbulence studies

On the basis of the NS eq. (I.2) one can derive an infinite system of equations for the moments of the velocity field, which has been investigated using various hypotheses with respect to closing the chain of equations by expressing higher correlation functions in terms of lower ones: the hypotheses about spectral energy transfer [2], i.e., expressing the third moment through the second one; Millionshchikov’s hypothesis about splitting the fourth moments in second ones [20, 21, 2], etc. In practice, the nonlinearity is extremely strong in the Navier–Stokes equation, and there are no strict reasons for closing the chain of equations for the moments. The degree of accuracy of such approximations is completely vague; conservation of general symmetry properties of the equation and appeal to experiment can be taken as arguments. It is obvious that agreement with one of the experiments may be accidental, and the situation can become even worse, if we try to refine the approximation in which the higher moments are split [22, 23].

The modern statistical theory of hydrodynamic turbulence goes back to the papers by Kraichnan (1959) [24] and Wyld (1961) [25], who suggested to simulate excitation of stationary spatially homogeneous developed hydrodynamic turbulence with the help of a spatially distributed variable force $\psi(\mathbf{r}, t)$. According to the Kolmogorov–Obukhov universality hypothesis [1–5] one can believe that in the limit of a large Reynolds number, the properties of the fine-scale part of the turbulence (in the inertial range) will not depend on the way the turbulence is excited, i.e., on the type of boundary conditions for the liquid flow or characteristics of the exciting force $\psi(\mathbf{r}, t)$. Therefore, one can suppose that the force $\psi(\mathbf{r}, t)$ is a random force with Gaussian statistics. It does not excite a mean flow: $\langle \psi(\mathbf{r}, t) \rangle = 0$, and its pair correlation function D_{ij} depends only on the coordinates and the time difference,

$$\langle \psi_i(\mathbf{r}_1, t_1) \psi_j(\mathbf{r}_2, t_2) \rangle = D_{ij}(\mathbf{r}_1 - \mathbf{r}_2, t_1 - t_2). \quad (\text{I.16})$$

This formula is the condition that the turbulence excitation be stationary and homogeneous. On the other hand, one should warn against arbitrary assumptions on the properties of $D(\mathbf{R}, \tau)$: it follows from physical considerations that there is no forced excitation of turbulence in the inertial range. Therefore,

the correlation function $D(R, \tau)$ must be concentrated in the region $R \geq L_{\text{ext}}, \tau > L_{\text{ext}}/V_T$, where $V_T = \langle |v(r, t)|^2 \rangle^{1/2}$ is the mean square turbulence velocity.

The next principal step, conventional in investigations (see the monograph [2]), is to go over to the k -representation, that is, expand the turbulent fluid velocity field in plane waves. Such an expansion is a long way from the intuitive knowledge of hydrodynamic turbulence as a system of interacting well-localized eddies. On the other hand, it will enable one to use the detailed and rather powerful techniques of diagrammatic analysis of the perturbation series in k -space.

The diagram technique suggested by Wyld in 1961 [25] has become a regular procedure for investigation of developed uniform turbulence. Wyld's diagram technique is very similar to Feynman's well-known diagram technique for quantum electrodynamics and for other field theories: the rules for reading the diagrams are the same in both techniques, the Dyson equations for the Green function are the same as well.

The principal feature of Wyld's technique (as well as of any technique for strongly nonequilibrium systems [26]) consists in the construction of two diagram series, one for the Green function (GF) $G_{ij}(\mathbf{k}, \omega)$ and one for the velocity pair correlation function $F_{ij}(\mathbf{k}, \omega)$,

$$G_{ij}(\mathbf{k}, \omega) \delta(\mathbf{k} - \mathbf{k}_1) \delta(\omega - \omega_1) = \lim_{f \rightarrow 0} \langle \delta v_i(\mathbf{k}, \omega) \delta f_j(\mathbf{k}, \omega) \rangle, \quad (\text{I.17})$$

$$F_{ij}(\mathbf{k}, \omega) \delta(\mathbf{k} - \mathbf{k}_1) \delta(\omega - \omega_1) = \langle v_i(\mathbf{k}, \omega) v_j^*(\mathbf{k}, \omega) \rangle. \quad (\text{I.18})$$

Here $v(\mathbf{k}, \omega)$ and $f(\mathbf{k}, \omega)$ are the velocity field $v(r, t)$ and external force $f(r, t)$ in the \mathbf{k}, ω representation. In thermodynamic equilibrium the functions G and D are related by a universal relationship (by the fluctuation-dissipation theorem [26]) and the two types of function reduce to one type. In turbulence there is no such universal relation.

Using his diagram technique, Wyld [25] demonstrated that the Direct Interaction Approximation (DIA) formulated by Kraichnan [24] corresponds to the approximation in which the vertices do not renormalize. In the theory of strong hydrodynamic turbulence as well as in the theory of phase transitions, however, the whole diagram series (renormalizing the interactions) should be taken into account. The degrees of agreement between various versions of hypotheses of scaling and the diagram series of Wyld's technique have been studied with regard to the above property by Kuzmin and Patashinsky [27].

The divergence of integrals in the range of both large and small momenta is one of the principal results in the investigation of the diagram series of scaling solutions. These integrals should be cut off at the momenta $1/L_{\text{ext}}$ and $1/L_{\text{int}}$ corresponding to the external and internal scales of turbulence, which thus enter the expression for the Green function and the velocity pair correlation function. Thus, the hypotheses of universality of turbulence for $\text{Re} \rightarrow \infty$ and its locality in the inertial interval are questionable. These problems are principal in the theory of developed turbulence. Kraichnan [24] was the first to mention IR divergence of the first diagram in the series for mass operators.

Kadomtsev [28] and Kraichnan [29] associated those divergences with the kinematic effect of sweeping of the k -eddies as a whole by an almost uniform velocity field V_T of large vortices of size L_{ext} . This sweeping is characterized by the Doppler frequency kV_T , which exceeds the Kolmogorov frequency $\gamma(k)$, eq. (I.10c), characterizing the local dynamic interaction of k -eddies, by a factor $(kL)^{1/3}$.

IR divergence in Kraichnan's DIA led to the following erroneous energy spectrum in the inertial

interval [24]:

$$E(k) \simeq (\varepsilon v_T / \rho)^{1/2} k^{-3/2} \simeq (\varepsilon / \rho)^{2/3} k^{-5/3} (kL_{\text{ext}})^{-1/6}. \quad (\text{I.19})$$

The spectrum (I.19) differs from the KO spectrum (I.9) by the factor $(kL_{\text{ext}})^{-1/6}$. The reason for this difficulty is that DIA does not separate the sweeping and dynamic interactions correctly. Therefore, the problem consists in distinguishing and studying a relatively weak dynamic γ -interaction that determines the turbulence spectrum in the formal technique of the theory (e.g. in Wyld's diagram technique [25]) on the background of the effect of kV_T -sweeping masking the interaction. The natural way to solve this problem is to use, for the description of the dynamic interaction of eddies, variables without the kinematic effect of sweeping. Kraichnan [29] used the Lagrange description of fluid flows for this purpose, but this led to serious technical difficulties, which did not allow him to go further than the direct interaction approach.

The authors of a number of papers [28, 30–34] tried to solve this problem by the explicit introduction of a separation scale, k' , into the theory, $L_{\text{ext}}^{-1} < k' < k$. Unfortunately, in so doing sweeping of k -eddies by significantly larger k' -eddies is always kept and the difficulties in the theory remain. The present author [35] suggested a method for the separation of the kinematic effect of sweeping and the dynamic interaction without using a separation scale. This technique, the so-called “internal diagram technique”, is based on a representation of the Green function and the velocity pair correlation function in which the term kV_T responsible for the sweeping is explicitly extracted from the mass operator $\Sigma(k, \omega)$; it seems that their difference would describe only the dynamic interaction and contain no infrared divergences associated with the sweeping.

In refs. [37, 36], in the scope of the internal diagram technique in Euler variables, it is shown that in the “direct dynamic interaction approximation” corresponding to taking only one diagram in the internal diagram technique into account divergences are absent. This approach is much better than Kraichnan's direct interaction approach [24] because it takes accurately into account the effect of sweeping in every order of perturbation theory, while the rather weak effect of the dynamic interaction of eddies is considered approximately, by the first diagram of the internal diagram technique. Unfortunately, a simple analysis of some diagrams of fourth order in the vertices in the internal diagram technique in Euler variables reveals logarithmic divergences.

The problem of eliminating sweeping in all orders of perturbation theory was solved by Belinicher and the present author in ref. [38] with the help of a transition to a moving reference system associated with the fluid velocity in some reference point of space r_0 . The physical ideas about this way of developing a consistent theory of turbulence will be discussed in this work, which presents the scale-invariant theory of developed hydrodynamic turbulence constructed in terms of the Hamiltonian equations of motion for the Clebsch variables.

This paper consists of two parts: a physical introduction and a mathematical supplement. The first part discusses at a qualitative level the problem of describing developed hydrodynamic turbulence using Wyld's diagram technique for the Navier–Stokes equations, describes some of the difficulties encountered by the theory, formulates physical ideas to overcome them and shows how this is done in the present work. It also describes some of the physical results obtained in these studies.

The second part formulates the mathematical methods of the theory: the momentum-nondiagonal diagram technique, presents a proof of the IR and UV convergence of all the diagrams, as well as a derivation of the solutions of the diagram equations for the Green function and the pair correlation

function describing Kolmogorov-type hydrodynamic turbulence, examines the structure of these functions and gives calculations of their asymptotic behavior. This part is intended for researchers who are interested in the technical details of the theory presented here. In a first reading it may be skipped by those interested mainly in the physical aspects of the problem of the description of turbulence.

The conclusion formulates briefly the results and some of the problems facing the statistical theory of turbulence using the method of perturbation theory in the dynamic interaction amplitudes.

Finally I would like to note that many interesting papers deal with closure problems (like Kraichnan's DIA [24, 29], Effinger and Grossmann's method of reduction of the correlation function [34] and so on), with the renormalization group approach to the theory of turbulence [39–55], with vortex dynamics (see, for example, refs. [56–59]), which remain out of our discussion here.

PART I. PHYSICAL INTRODUCTION TO THE THEORY, RESULTS AND DISCUSSION

1. The problem of eliminating the sweeping interaction in the theory of turbulence

1.1. *Dynamic and sweeping interactions*

As we discussed before, the problem of developed hydrodynamic turbulence of an incompressible fluid involves two essentially different interactions. The first one is the *dynamic* interaction of turbulent fluid motions with the characteristic spatial scale $1/k$ (more specifically called *k-eddies*). This interaction leads to energy exchange between the *k-eddies* with characteristic frequency $\gamma(k)$, eq. (I.10c). The other interaction is the *sweeping* interaction (or simply sweeping of small *k-eddies*, without any shape variations!) by a spatially uniform part of a turbulent field of velocity $\mathbf{v}(\mathbf{r}, t)$. Here \mathbf{r} is the coordinate of the “center of gravity” of the *k-eddy*. Sweeping is characterized by the Doppler frequency $\omega_D(\mathbf{k}) \simeq kV_T$, where V_T is the mean square velocity. It should be stressed that the given definition of the sweeping interaction differs from the conventional understanding of sweeping *processes*. The latter ones always involve some shape distortion of *k-eddies* in the sweeping process due to spatial nonuniformity of a real turbulent velocity field $\mathbf{v}(\mathbf{r}, t)$. According to our definition, this shape distortion contributes to the above-mentioned dynamic interaction. Thus a complete sweeping process includes both interactions.

Let us consider a model situation in which there are only two groups of eddies (k_1 -eddies and k_2 -eddies) with different scales ($k_1 \ll k_2$) and velocities of motion V_1 and V_2 , which correspond to the Kolmogorov–Obukhov energy scale distribution (the *turbulence spectrum*). The sweeping interaction of these groups of eddies is described by the term $(V_1 \cdot \nabla)V_2$ in the Euler equation (I.1) and is characterized by the Doppler frequency $\omega_D(k_1, k_2) = k_2 V(k_1)$. The dynamic distortion of small k_2 -eddies is defined by the term $(V_2 \cdot \nabla)V_1$ and is characterized by the frequency $\gamma(k_1, k_2) \simeq k_1 V(k_1)$. According to the eq. (I.10a), the characteristic *k-eddy* velocity $V(k) \simeq (\varepsilon/\rho k)^{1/3}$. This gives an estimate for the characteristic frequencies of interactions of k_2 -eddies,

$$\gamma(k_1, k_2) \simeq (\varepsilon/\rho)^{1/3} k_1^{2/3}, \quad \text{for } k_1 \ll k_2, \quad (1.1)$$

$$\omega_D(k_1, k_2) \simeq (\varepsilon/\rho)^{1/3} k_1^{-1/3} k_2, \quad \text{for } k_1 \ll k_2. \quad (1.2)$$

It is seen that the contribution of large k_1 -eddies to the dynamics of small k_2 -eddies increases when k_1

approaches k_2 . The dynamic interaction is most efficient for eddies of the same scale. This statement is essentially Kolmogorov's hypothesis of locality of the dynamic interactions of eddies in \mathbf{k} -space.

The sweeping interaction behaves in an inverse manner as compared to the dynamic one. The contribution of large k_1 -eddies to sweeping of small k_2 -eddies grows with the size of the former and is maximal in the energy-containing range for $k_1 \approx \min k_1 \approx 1/L$. Compare the maximal (in k_1) interaction frequencies of k_2 -eddies,

$$\max \gamma(k_1, k_2) = \gamma(k_2, k_2) = \gamma(k_2) \approx (\varepsilon/\rho)^{1/3} k_2^{2/3}, \quad (1.3a)$$

$$\max \omega_D(k_1, k_2) = \omega(1/L, k_2) = \omega_D(k_2) \approx (\varepsilon/\rho)^{1/3} k_2 L^{1/3}, \quad L = L_{\text{ext}}, \quad (1.3b)$$

$$\omega_D(k_2) \approx \gamma(k_2)(k_2 L)^{1/3} \gg \gamma(k_2). \quad (1.3c)$$

It is seen that the sweeping interaction [with frequency $\omega_D(k_2)$] is substantially stronger than the dynamic one [with frequency $\gamma(k_2)$]. But the sweeping interaction does not contribute to the energy change of k -eddies. This is merely the kinematic effect of their traveling in \mathbf{r} -space as an entity.

1.2. Sweeping interaction and infrared divergences

We have clarified above that the dynamic interaction completely determines the spectrum of turbulence and is much weaker than the sweeping interaction. The latter is, however, also a real physical effect; therefore it also appears in equations of the theory, masking the dynamic interaction and radically hindering its investigation. There were numerous attempts to eliminate sweeping from the formal apparatus of the theory [28–33]. They have clarified the structure of the theory and led to a better understanding of the problems. The pioneering works of Kraichnan [24], Wyld [25] and Kadomtsev [28] have shown that sweeping results in infrared (IR) divergences of integrals in the Wyld diagrams for the pair correlation function of the velocity and the Green functions. My preprint ref. [35] (see also the review [37] and ref. [36]) gives an analysis of the divergences and formulates the *sweeping approximation*, which takes into consideration only the most divergent part in each diagram. In this approximation, one can carry out an exact summation of the diagram series to find the frequency dependences of the Green function $G(\mathbf{k}, \omega)$ and the pair correlation function $F(\mathbf{k}, \omega)$ in the inertial range,

$$G(\mathbf{k}, \omega) = \langle [\omega - \mathbf{k} \cdot \mathbf{v}(\mathbf{r}_0, t) + i0]^{-1} \rangle = (1/kV_T)g(\omega/kV_T), \quad (1.4a)$$

$$F(\mathbf{k}, \omega) = F(\mathbf{k})\langle \delta(\omega - \mathbf{k} \cdot \mathbf{v}(\mathbf{r}_0, t)) \rangle = [F(\mathbf{k})/kV_T]f(\omega/kV_T). \quad (1.4b)$$

The functions $g(x)$ and $f(x)$ are determined by the statistical characteristics of turbulence in the energy-containing range and are not universal. The function $F(\mathbf{k})$, which determines the spectrum of turbulence $E(k)$, eq. (I.7), remains random in the sweeping approximation. This is due to the fact that it disregards the dynamic interaction. The less divergent (in the IR range) integrals omitted in the sweeping approximation are $\gamma(k)/kV_T \approx (kL)^{-1/3}$ times as small.

Thus there remains the problem to determine the turbulence spectrum and the closely related problem of IR divergences. We shall deal with several questions. The first is: Are the IR divergences only due to the sweeping interaction? In other words: Will the IR divergences remain after complete

elimination of sweeping from the theory? Are there any other physical reasons for the IR divergences similar to intermittency? Recall that intermittency in developed turbulence is generally understood as the non-Gaussian behavior of the statistical characteristics of k -eddies increasing with k (see, for example, ref. [2]). But does intermittency really exist in this sense? If it does, then how to describe it based on the Navier–Stokes equation?

1.3. In which region is it really necessary to eliminate sweeping?

The first step in solving the questions mentioned in the previous subsection should be elimination of the sweeping interaction from the formal apparatus of the theory. A natural way to do this is to use variables in which the sweeping interaction is absent. For that purpose Kraichnan [29] suggested the use of Lagrangian variables $\mathbf{u}(\mathbf{r}, t_0, t)$, i.e., the velocities of fluid particles which at the moment t_0 were in point \mathbf{r} . Knowing these velocities, it is easy to find trajectories of the particles,

$$\mathbf{r}(t) = \mathbf{r} + \int_{t_0}^t \mathbf{u}(\mathbf{r}, t_0, \tau) d\tau. \quad (1.5)$$

Evidently, the Lagrangian velocity coincides with the Eulerian velocity $\mathbf{v}(\mathbf{r}, t)$ if one takes the trajectory $\mathbf{r}(t)$ for \mathbf{r} ,

$$\mathbf{u}(\mathbf{r}, t_0, t) = \mathbf{v}\left(\mathbf{r} + \int_{t_0}^t \mathbf{u}(\mathbf{r}, t_0, \tau) d\tau, t\right). \quad (1.6)$$

Regretfully, Wyld's diagram technique for the Lagrangian velocity proved to be very complicated and Kraichnan did not manage to come essentially further in his theory than the direct interaction approximation [29].

It should be emphasized that the Lagrangian approach eliminates the sweeping interaction *in the whole region* of turbulent motion of a fluid. Actually, complete elimination of sweeping in the whole region is superfluous and is not necessary for building a theory free from sweeping effects. In the work of Belinicher and myself [38] it is proved that, in order to eliminate the sweeping interactions from the diagram series of the perturbation theory describing the turbulence of small k -eddies ($kL \gg 1$), it is enough to eliminate it in a limited region with the characteristic spatial extent (*scale*) $l(k)$ of the order of $1/k$.

Let us discuss some physical considerations helping to understand this statement. First of all, $l(k)$ should not exceed the energy-containing scale L . This is so because L is the scale of the largest eddies in a system, and the long-range fluid motion is statistically independent. Therefore the theory of spatially uniform turbulence should not be built on the whole space. It is sufficient to do this in a limited region of scale L .

In order to admit the possibility to make $l(k)$ smaller than L , recall Kolmogorov's hypothesis on the locality of the dynamic interactions of eddies in k -space: the dynamics of k -eddies is mainly determined by their interactions with k_1 -eddies of the same scale. Consider a specified k -eddy located in a region of scale $1/k$ surrounding the point \mathbf{r}_0 . The k_1 -eddies efficiently interacting with it are located in a region of scale $\lambda(k)$ surrounding the same point. Here $\lambda(k)$ is the characteristic range of interaction (*interaction length*) of two eddies of the same scale $1/k$. These eddies are involved in the same cascade decay process of the initial $1/L$ -eddy of the energy-containing scale L . In principle, this might lead to their

phase coherence and their enhanced interaction at long distances up to L . If such long-range interactions were essential, sweeping should have been excluded in the whole region of scale L occupied by the entire cascade. However, in agreement with Kolmogorov's suggestion (and the conventional viewpoint), the dynamic characteristics of the initial $1/L$ -eddy (such as the phase of the motion) are "forgotten" in the stage-by-stage decay process. As a result, in the limit where the "cascade stage number" is large, the coherence and long-range interaction of k -eddies should disappear. Thus the interaction length of k -eddies $\lambda(k)$ should be of the order of their geometric size $1/k$. This statement represents the hypothesis of the locality of eddy interactions in r -space. This and Kolmogorov's hypothesis about the locality of dynamic interactions in k -space show that the study of the asymptotic stages of the energy cascade (in the limit $kL \rightarrow \infty$) may be restricted to investigation of only one of its stages, which is reiterated in the cascade in a self-similar way. This stage involves the k -eddies located in a limited region of scale $\lambda(k) \approx 1/k$, in which case the effect of other eddies of the cascade is defined by self-consistent parameters such as the energy flux over the spectrum ε , the number of the cascade stage kL , etc. As a result, we arrive at the above-mentioned statement about elimination of sweeping being sufficient in a limited region of scale $1/k$.

2. Quasi-Lagrangian method of local elimination of the sweeping interaction

To eliminate the sweeping in the required limited region, the so-called *quasi-Lagrangian velocity* $\mathbf{u}(\mathbf{r}_0, \mathbf{r}, t_0, t)$ was suggested by me in 1980 (see the review [37]). This velocity may be defined from eq. (1.6). For that purpose it is necessary to replace in the integrand the velocities $\mathbf{u}(\mathbf{r}, t_0, \tau)$ of the particles in the region we are considering by the velocity of one of them, say, by $\mathbf{u}(\mathbf{r}_0, t_0, \tau)$. We shall call this specified point with coordinate \mathbf{r}_0 the *marker point*. The resulting equation is easily rewritten as

$$\mathbf{v}(\mathbf{r}, t) = \mathbf{u}\left(\mathbf{r}_0, \mathbf{r} - \int_{t_0}^t \mathbf{u}(\mathbf{r}_0, \mathbf{r}_0, t_0, \tau) d\tau, t\right). \quad (2.1)$$

Here the function $\mathbf{u}(\mathbf{r}_0, \mathbf{r}, t_0, t)$ has obtained an additional argument, the coordinate of the marker point \mathbf{r}_0 . If the velocities of all particles on our scale are identical, the velocity $\mathbf{u}(\mathbf{r}_0, \mathbf{r}, t_0, t)$ naturally coincides with the Lagrangian velocity of fluid particles along the actual trajectory. As the real velocities on our scale are nearly identical, the velocities $\mathbf{u}(\mathbf{r}_0, \mathbf{r}, t_0, t)$ will differ little from the Lagrangian ones. Therefore it would be reasonable to call them *quasi-Lagrangian* (qL) velocities.

It should be stressed that eq. (2.1) contains no approximations. All the above physical considerations reaffirm such a choice of variables as being reasonable, promising success for the theory which will make use of them. Formula (2.1) itself represents a precise relation between the Eulerian and quasi-Lagrangian velocities. The quasi-Lagrangian velocity is as much a physical reality as the Eulerian or Lagrangian velocity; it may be experimentally measured and effectively used in numerical turbulence modeling. In its terms one can adequately construct a theory of turbulence.

An equation for the qL velocity may be derived by substituting expression (2.1) into the Navier-Stokes equation,

$$\begin{aligned} \frac{\partial \mathbf{u}(\mathbf{r}_0, \mathbf{r}, t_0, t)}{\partial t} + \{[\mathbf{u}(\mathbf{r}_0, \mathbf{r}, t_0, t) - \mathbf{u}(\mathbf{r}_0, \mathbf{r}_0, t_0, t)] \cdot \nabla\} \mathbf{u}(\mathbf{r}_0, \mathbf{r}, t_0, t) + \nabla p(\mathbf{r}_0, \mathbf{r}, t_0, t) \\ - \nu \Delta \mathbf{u}(\mathbf{r}_0, \mathbf{r}, t_0, t) = 0, \quad \text{div } \mathbf{u}(\mathbf{r}_0, \mathbf{r}, t_0, t) = 0. \end{aligned} \quad (2.2)$$

This equation differs from the Navier–Stokes one in the underlined term subtracting sweeping in the marker point \mathbf{r}_0 . Sweeping persists in all other points $\mathbf{r} \neq \mathbf{r}_0$.

We shall now estimate the dimension of the region $l(k)$ where the residual sweeping interaction of k -eddies is smaller than the dynamic one. For that purpose compare their characteristic frequencies $\gamma(k)$ and $k \delta v(l)$. Here $\delta v(l)$ is the residual sweeping velocity in a region of scale l ,

$$\delta v(l) = \langle [\mathbf{v}(\mathbf{r}_0 + l, t) - \mathbf{v}(\mathbf{r}_0, t)]^2 \rangle^{1/2}. \quad (2.3)$$

The main contribution to this velocity is made by the $1/l$ -eddies; therefore

$$\delta v(l) \simeq (\varepsilon l / \rho)^{1/3}, \quad k \delta v(l) \sim k (\varepsilon l / \rho)^{1/3}. \quad (2.4)$$

Taking into account expression (1.3a) for $\gamma(k)$, we obtain from the condition $\gamma(k) = k \delta v(l)$ the following estimate for the scale $l(k)$ of the region where the sweeping interaction has been eliminated to the required approximation: $l(k) \simeq 1/k$. (It should be noted that this estimate of $l(k)$ might have been written at once, since in our treatment based on the Richardson–Kolmogorov–Obukhov view of turbulence, $1/k$ is the only quantity with the dimension of length.) Recall that for an effective description of the dynamic interaction of k -eddies it is necessary to eliminate sweeping exactly in such a region.

For the formal apparatus of the theory to make use of it, we should give up the idea of describing turbulence in the whole \mathbf{r} -space. For that purpose, the functions $G(\mathbf{k}, \omega)$ and $F(\mathbf{k}, \omega)$ (describing the *global* properties of turbulence) should in a new theory be replaced by the *local* characteristics $G(\mathbf{r}, \mathbf{k}, \omega)$ and $F(\mathbf{r}, \mathbf{k}, \omega)$ defining the properties of turbulence in point \mathbf{r} . Now we shall discuss, how this is determined.

3. Local statistical characteristics $G(\mathbf{r}, \mathbf{k}, \omega)$ and $F(\mathbf{r}, \mathbf{k}, \omega)$ of the turbulent velocity field

First of all, it is necessary to introduce in a traditional way, in the ω, \mathbf{k} representation, the Green function G and the pair correlation function for the quasi-Lagrangian velocity F ,

$$G_{ij}(\mathbf{r}_0, \mathbf{k}_1, \mathbf{k}_2, \omega_1) \delta(\omega_1 - \omega_2) = \langle \delta u_i(\mathbf{r}_0, \mathbf{k}_1, t_0, \omega_1) / \delta f_j(\mathbf{r}_0, \mathbf{k}_2, t_0, \omega_2) \rangle, \quad (3.1a)$$

$$F_{ij}(\mathbf{r}_0, \mathbf{k}_1, \mathbf{k}_2, \omega_1) \delta(\omega_1 - \omega_2) = \langle u_i(\mathbf{r}_0, \mathbf{k}_1, t_0, \omega_1) u_j^*(\mathbf{r}_0, \mathbf{k}_2, t_0, \omega_2) \rangle, \quad (3.1b)$$

$$\mathbf{u}(\mathbf{r}_0, \mathbf{k}, t_0, \omega) = \int \mathbf{u}(\mathbf{r}_0, \mathbf{r}, t_0, t) \exp[i(\omega t - \mathbf{k} \cdot \mathbf{r})] d\mathbf{r} dt. \quad (3.2)$$

Here $\mathbf{u}(\mathbf{r}_0, \mathbf{k}, t_0, \omega)$ is the qL velocity in the ω, \mathbf{k} representation, angular brackets denote turbulent ensemble averaging, and f is an external force. Equation (2.2) does not contain the marker time t_0 in explicit form. Therefore the Green function and the pair correlation function for the qL velocity, like these quantities for the Eulerian velocity, are invariant relative to a time shift. As a result, the functions (3.1) are independent of t_0 and proportional to $\delta(\omega_1 - \omega_2)$. The main difference between the quasi-Lagrangian and the conventional (in terms of the Eulerian velocity) description of turbulence is that the wave vector \mathbf{k} is no longer preserved and the functions (3.1) become nondiagonal in \mathbf{k} [i.e., not

proportional to $\delta(\mathbf{k}_1 - \mathbf{k}_2)$]. This is a result of the absence of spatial uniformity of the theory due to the explicit dependence of the equations of motion on the coordinate of the marker point \mathbf{r}_0 in which sweeping is precisely eliminated.

Now we introduce the mixed $\mathbf{r}, \omega, \mathbf{k}$ representation,

$$\phi(\mathbf{r} - \mathbf{r}_0, \mathbf{k}, \omega) = \int \exp(i\mathbf{s} \cdot \mathbf{r}) \phi(\mathbf{r}_0, \mathbf{k} + \mathbf{s}/2, \mathbf{k} - \mathbf{s}/2, \omega) d\mathbf{s}. \quad (3.3)$$

Here ϕ is any of the functions G or F . In this method of introducing the \mathbf{r} representation the functions $G(\mathbf{r}, \mathbf{k}, \omega)$ and $F(\mathbf{r}, \mathbf{k}, \omega)$ have the above-mentioned physical sense. They actually describe the statistical properties of k -eddies in a region of scale $1/k$ surrounding the point \mathbf{r} . The symmetric method (3.3) to determine the quasilocal characteristics of a field is the usual method in theoretical physics. It is used, for example, in studying electrons and photons in spatially nonuniform solids.

Now we shall discuss the general properties of the functions G and F in the quasi-Lagrangian approach. It follows from the definitions (2.1) and (3.2) of the quasi-Lagrangian velocity that the dependence of the functions G and F , eq. (3.1), on \mathbf{r}_0 is universal,

$$G(\mathbf{r}_0, \mathbf{k}_1, \mathbf{k}_2, \omega) = G(\mathbf{k}_1, \mathbf{k}_2, \omega) \exp[i(\mathbf{k}_1 - \mathbf{k}_2) \cdot \mathbf{r}_0], \quad (3.4a)$$

$$F(\mathbf{r}_0, \mathbf{k}_1, \mathbf{k}_2, \omega) = F(\mathbf{k}_1, \mathbf{k}_2, \omega) \exp[i(\mathbf{k}_1 - \mathbf{k}_2) \cdot \mathbf{r}_0]. \quad (3.4b)$$

The quantities G and F on the right-hand sides of eqs. (3.4) are the values of these functions at $\mathbf{r}_0 = 0$. It also follows from this and from the form of the integral transformation (3.3) that in the \mathbf{r}, \mathbf{k} representation, the functions G and F depend only on the difference between the coordinates $\mathbf{r} - \mathbf{r}_0$ and not on each of them separately. This is a consequence of the spatial uniformity of developed turbulence.

The quantities G and F are determined by formulas (3.1) in the ω representation. In the t representation, we have instead of (3.1b)

$$F_{ij}(\mathbf{r}_0, \mathbf{k}_1, \mathbf{k}_2, t_1 - t_2) = \langle u_i(\mathbf{r}_0, \mathbf{k}_1, t_0, t_1) u_j^*(\mathbf{r}_0, \mathbf{k}_2, t_0, t_2) \rangle, \quad (3.5a)$$

$$F_{ij}(\mathbf{r}_0, \mathbf{k}_1, \mathbf{k}_2, \tau) = \int F_{ij}(\mathbf{r}_0, \mathbf{k}_1, \mathbf{k}_2, \omega) \exp(-i\omega\tau) d\omega/2\pi. \quad (3.5b)$$

The one-time correlation function $F_{ij}(\mathbf{r}_0, \mathbf{k}_1, \mathbf{k}_2) = F_{ij}(\mathbf{r}_0, \mathbf{k}_1, \mathbf{k}_2, 0)$ may be calculated at any time $t_1 = t_2$, in particular, at $t_1 = t_2 = t_0$. But it follows from formula (2.1) that at $t = t_0$ the quasi-Lagrangian velocity coincides with the Euler velocity and does not depend on \mathbf{r}_0 . Therefore the one-time correlation function of the quasi-Lagrangian velocity $F_{ij}(\mathbf{r}_0, \mathbf{k}_1, \mathbf{k}_2)$ does not depend on \mathbf{r}_0 and is diagonal in $\mathbf{k}_1, \mathbf{k}_2$,

$$\int F_{ij}(\mathbf{r}_0, \mathbf{k} + \mathbf{s}/2, \mathbf{k} - \mathbf{s}/2, \omega) d\omega/2\pi = F_{ij}(\mathbf{k})\delta(\mathbf{s}). \quad (3.6)$$

This integral relation is extremely important. It will allow us, after we have constructed the theory in the quasi-Lagrangian variables, to calculate the one-time correlation functions of the Euler velocity.

4. Scale invariant limit in the theory of fully developed turbulence

Let us recall that the characteristic frequencies of the dynamic and sweeping interactions of k -eddies depend differently on k [see, e.g., eq. (1.3)]. As a result, their ratio depends on the scale $1/k$ of eddies and the theory of turbulence in the Euler variables cannot be scale invariant. In order to make such a formulation possible, one should eliminate the sweeping interaction. The scale invariant formulation of the theory of turbulence in the limit $kL \rightarrow \infty$ based on eq. (2.2) for the quasi-Lagrangian velocity (2.1) was suggested in 1986 by Belinicher and myself [38, 60]. Following Wyld, we have constructed, in terms of perturbation theory, the diagram equations for $F(\mathbf{r}, \mathbf{k}, \omega)$ and $G(\mathbf{r}, \mathbf{k}, \omega)$. We have proved that all integrals in every diagram of every order with respect to vertices converge both in the IR and UV regions. Therefore in these integrals one may set $k_{\min} = 1/L_{\text{ext}} = 0$ and $k_{\max} = 1/L_{\text{int}} = \infty$ (L_{int} is the internal turbulence scale defined by the viscosity). Thus the dimensional quantities L_{ext} and L_{int} vanish in this limit of our theory, which assumes a scale invariant form.

It is important to note that, due to convergence of the integrals in the quasi-Lagrangian approach, the equations for $G(\mathbf{r}, \mathbf{k}, \omega)$ and $F(\mathbf{r}, \mathbf{k}, \omega)$ really describe only one stage of the energy cascade which involves the k -eddies from the region of size $1/k$ surrounding the point \mathbf{r}_0 . The proof of the convergence of the integrals in these equations is essentially a proof of the locality of the dynamic interaction in \mathbf{r} - and \mathbf{k} -space.

The most important result of the scale invariant theory of turbulence is the following: in the limit $\text{Re} \rightarrow \infty$, the scale invariant solution of the diagram equations has been obtained where the scaling index of the vertices is not renormalized. This solution is consistent with the Richardson–Kolmogorov–Obukhov picture of turbulence, where there is no intermittency in the traditional sense.

5. Hamiltonian approach to the theory of turbulence of an incompressible fluid

5.1. Canonical equations of motion

We shall proceed from the Euler equations written in canonical form [61–63],

$$\partial \lambda / \partial t = \delta H / \delta \mu, \quad \partial \mu / \partial t = -\delta H / \delta \lambda. \quad (5.1)$$

Here the Hamiltonian H represents the kinetic energy expressed via the Clebsch canonical variables $\lambda(\mathbf{r}, t)$ and $\mu(\mathbf{r}, t)$,

$$H = (\rho/2) \int |\mathbf{v}(\mathbf{r}, t)|^2 d\mathbf{r}, \quad \mathbf{v} = \lambda \nabla \mu - \nabla \phi. \quad (5.2)$$

The potential $\phi(\mathbf{r}, t)$ is determined from the incompressibility condition $\text{div } \mathbf{v} = 0$.

The Clebsch variables describe a particular but physically important class of flows in which the eddy lines are the intersection lines of two families of surfaces $\lambda(\boldsymbol{\gamma}, t) = C_1$ and $\mu(\mathbf{r}, t) = C_2$. These surfaces stratify the space and move together with the fluid. For example, the Clebsch variables may describe the turbulence arising from the instability of plane-parallel or axially symmetric Couette flow. In the general case these variables may be introduced locally.

It is convenient to go over from the pair of real variables λ and μ to the complex ones a and a^* ,

$$a(\mathbf{r}, t) = [\lambda(\mathbf{r}, t) + i\mu(\mathbf{r}, t)]/\sqrt{2}.$$

In these variables eqs. (5.1) and (5.2), after transition to the \mathbf{k} -representation, have the form

$$i \partial a(\mathbf{k}, t) / \partial t = \delta H / \delta a^*(\mathbf{k}, t), \quad (5.3)$$

$$H = (\rho/4) \int T_{12,34} a_1^* a_2^* a_3 a_4 d\mathbf{k}_1 d\mathbf{k}_2 d\mathbf{k}_3 d\mathbf{k}_4, \quad a_j = a(\mathbf{k}_j, t), \quad (5.4a)$$

$$T_{12,34} = T(\mathbf{k}_1, \mathbf{k}_2; \mathbf{k}_3, \mathbf{k}_4) = \rho(\psi_{13} \cdot \psi_{24} + \psi_{14} \cdot \psi_{23}) \delta(\mathbf{k}_1 + \mathbf{k}_2 - \mathbf{k}_3 - \mathbf{k}_4), \quad (5.4b)$$

$$\psi_{ij} = \psi(\mathbf{k}_i, \mathbf{k}_j) = \frac{1}{2(2\pi)^{3/2}} \left(\mathbf{k}_i + \mathbf{k}_j - (\mathbf{k}_i - \mathbf{k}_j) \frac{k_i^2 - k_j^2}{|\mathbf{k}_i - \mathbf{k}_j|^2} \right). \quad (5.4c)$$

In these terms the fluid velocity in the \mathbf{k} representation reads

$$\mathbf{v}(\mathbf{k}, t) = -i \int \psi_{12} a_1^* a_2 \delta(\mathbf{k} + \mathbf{k}_1 - \mathbf{k}_2) d\mathbf{k}_1 d\mathbf{k}_2. \quad (5.5)$$

It should be pointed out that the ‘‘turbulence Hamiltonian’’ (5.4) includes only the four-particle interaction Hamiltonian $H = H_4$. It has no two-particle term of the type $H_2 \sim \omega a a^*$ describing the noninteracting field. Thus the dimensionless interaction quantity H_4/H_2 is equal to infinity (or to Re with viscosity considered). From the theoretical viewpoint, investigation of turbulence is a many-body problem involving exceedingly strong interactions.

5.2. Are the Hamiltonian and traditional approaches to the theory of turbulence equivalent?

We shall now discuss the following situation in the study of turbulence. In the Belinicher–L’vov theory (briefly discussed above) [38, 60] using natural variables (the fluid velocity), the Kolmogorov–Obukhov solution without intermittency has been obtained. An essentially different view of turbulence is presented in ref. [64] by Tur and Yanovsky, who adopt the Hamiltonian approach to the theory. They indicate the terms in their solution which are responsible for intermittency (for details see section 8.2 of this paper). This gives rise to the following possibilities: either this discrepancy is due to some errors or inaccuracies in refs. [38] and [64], or there are more serious reasons for it, associated with the differences between the two approaches to the theory of turbulence [the former is the traditional approach employing natural variables, the fluid velocity $\mathbf{v}(\mathbf{r}, t)$ or $\mathbf{u}(\mathbf{r}_0, r, t_0)$, and the latter is the Hamiltonian approach employing Clebsch variables].

The simplest choice between these alternatives is to state that there are no radical differences between the two approaches to the study of turbulence, and that it is only important to apply them correctly. However, this standpoint is more controversial than it may seem. Indeed, the canonical equations (5.1), (5.2) describe a particular class of flows, those without helicity. As to the Euler equations, they define flows with any type of helicity. The Eulerian velocity is quadratic in the Clebsch variables [see eqs. (5.5)]. Therefore the diagram series of Wyld’s perturbation theory for the Clebsch variables essentially differ from those for the Eulerian velocity. These two types of series are related by deep resummations which are sometimes difficult to find. Moreover, the diagram series in the theory of turbulence lack a small dimensionless parameter constructed from dimensional quantities (like the fine

structure constant $\alpha = 2\pi e^2/\hbar c \simeq 1/137$ in quantum electrodynamics). These are formal series, for which the summation procedure has not been mathematically established. Therefore, in principle, the use of these different approaches may lead to physically different solutions (e.g., with intermittency and without it).

Due to this, it is very interesting and important to carry out a comparative investigation of fully developed turbulence in the context of one and the same set of physical suggestions and ideas and employing both the Eulerian velocity and the Clebsch variables.

6. Formulation of the Hamiltonian theory of the dynamic interaction of eddies

Important steps in comparative turbulence studies in the traditional and Hamiltonian approaches are, first, elimination of the sweeping interaction; second, formulation of the diagram equations describing only the dynamic interaction of k -eddies; third, proving the convergence or examining the nature of the divergence of integrals in the diagrams, then finding solutions of the equations (in the context of certain physical hypotheses about the behavior of the series as a whole); and, finally, analysis of these solutions. This program in the traditional approach employing natural variables (velocity) has been realized by Belinicher and myself in ref. [38]. Its realization in the Hamiltonian approach is the main purpose of this work. The following subsection describes the first step.

6.1. Elimination of the sweeping interaction

In line with the idea of the quasi-Lagrangian approach and in analogy with formula (2.1), we determine the *Clebsch quasi-Lagrangian* variables $b(\mathbf{r}_0, \mathbf{r}, t_0, t)$ by the equation

$$a(\mathbf{r}, t) = b\left(\mathbf{r}_0, \mathbf{r} - \int_{t_0}^t \mathbf{u}(\mathbf{r}_0, \mathbf{r}_0, t_0, \tau) d\tau, t_0, t\right). \quad (6.1)$$

In the k representation we have

$$a(\mathbf{k}, t) = b(\mathbf{r}_0, \mathbf{k}, t_0, t) \exp\left(-i\mathbf{k} \int_{t_0}^t \mathbf{u}(\mathbf{r}_0, \mathbf{r}_0, t_0, \tau) d\tau\right). \quad (6.2a)$$

Expressing sequentially the velocity $\mathbf{u}(\mathbf{r}_0, \mathbf{r}, t_0, \tau)$ in the Eulerian velocity \mathbf{v} according to formula (2.1), \mathbf{v} in a and a^* by formula (5.5) and then a and a^* in b and b^* by formula (6.2a), we obtain

$$\mathbf{u}(\mathbf{r}_0, \mathbf{r}_0, t_0, \tau) = -i \int \psi_{12} b_1^* b_2 \exp[i(\mathbf{k}_1 - \mathbf{k}_2) \cdot \mathbf{r}_0] d\mathbf{k}_1 d\mathbf{k}_2, \quad \psi_{12} = \psi(\mathbf{k}_1, \mathbf{k}_2), \quad b_j = b(\mathbf{r}_0, \mathbf{k}_j, t_0, \tau). \quad (6.2b)$$

Formulae (6.2) provide a closed relation between the old canonical variables a, a^* and the new (quasi-Lagrangian) ones b, b^* . This change of variables is precise and contains no approximations, like formula (2.1) for the natural variables \mathbf{v} and \mathbf{u} . Earlier, in refs. [32, 33, 64], a similar procedure to eliminate the sweeping interaction was proposed and used, which was called by the authors *subtraction*

of zero modes. I do not now know how to explain the use of this term, but I note that their change of variables is obtained from (6.2) if we set $\mathbf{r}_0 = 0$ and substitute in the integrand in (6.2a) the function $\mathbf{t}u(\mathbf{r}_0, \mathbf{r}, t, \tau)$ for the constant $\mathbf{u}(\mathbf{r}_0, \mathbf{r}_0, t_0, t)$. The following section describes the second, very simple step of our program.

6.2. Derivation of the equations of motion for b and b^*

Substituting formulae (6.2), which directly express the Clebsch variables a and a^* in $b(\mathbf{r}_0, \mathbf{k}, t_0, t)$ and $b^*(\mathbf{r}_0, \mathbf{k}, t_0, t)$, into the canonical equations (5.3), (5.4) for a and a^* , we obtain

$$i \frac{\partial b(\mathbf{r}_0, \mathbf{k}, t_0, t)}{\partial t} = \frac{1}{2} \int W(\mathbf{r}_0, \mathbf{k}, \mathbf{k}_1; \mathbf{k}_2, \mathbf{k}_3) b_1^* b_2 b_3 d\mathbf{k}_1 d\mathbf{k}_2 d\mathbf{k}_3. \quad (6.3)$$

These equations differ from eqs. (5.3), (5.4) in the replacement of the vertex $T(\mathbf{k}, \mathbf{k}_1; \mathbf{k}_2, \mathbf{k}_3)$, eq. (5.4b), by $W(\mathbf{r}_0; \mathbf{k}, \mathbf{k}_1; \mathbf{k}_2, \mathbf{k}_3)$,

$$W(\mathbf{r}_0; \mathbf{k}, \mathbf{k}_1; \mathbf{k}_2, \mathbf{k}_3) = T(\mathbf{k}, \mathbf{k}_1; \mathbf{k}_2, \mathbf{k}_3) - T_s(\mathbf{r}_0; \mathbf{k}, \mathbf{k}_1; \mathbf{k}_2, \mathbf{k}_3) - T_s(\mathbf{r}_0, \mathbf{k}, \mathbf{k}_1; \mathbf{k}_3, \mathbf{k}_2), \quad (6.4a)$$

$$T_s(\mathbf{r}_0, \mathbf{k}, \mathbf{k}_1; \mathbf{k}_2, \mathbf{k}_3) = (2\pi)^{-3/2} (\mathbf{k} \cdot \boldsymbol{\psi}_{13}) \delta(\mathbf{k} - \mathbf{k}_2) \exp[i(\mathbf{k}_1 - \mathbf{k}_3) \cdot \mathbf{r}_0], \quad (6.4b)$$

$$\begin{aligned} W(\mathbf{r}_0; \mathbf{k}, \mathbf{k}_1; \mathbf{k}_2, \mathbf{k}_3) &= (2\pi)^{-3/2} \mathbf{k} \cdot [\boldsymbol{\psi}_{13} \{ \delta(\mathbf{k} + \mathbf{k}_1 - \mathbf{k}_2 - \mathbf{k}_3) - \delta(\mathbf{k} - \mathbf{k}_2) \exp[i(\mathbf{k}_1 - \mathbf{k}_3) \cdot \mathbf{r}_0] \} \\ &\quad + \boldsymbol{\psi}_{12} \{ \delta(\mathbf{k} + \mathbf{k}_1 - \mathbf{k}_2 - \mathbf{k}_3) - \delta(\mathbf{k} - \mathbf{k}_3) \exp[i(\mathbf{k}_1 - \mathbf{k}_2) \cdot \mathbf{r}_0] \}]. \end{aligned} \quad (6.4c)$$

We call the vertex T the *full* vertex (6.5c). It appeared first in eqs. (5.3), (5.4), which are equivalent to Euler's equations, and describes both the dynamic and sweeping interactions. The vertex T_s represents the asymptotic form of the full vertex T as $\mathbf{k} \rightarrow \mathbf{k}_2$ (or $\mathbf{k} \rightarrow \mathbf{k}_3$). It corresponds to the underlined term $[\mathbf{u}(\mathbf{r}_0) \cdot \nabla] \mathbf{u}(\mathbf{r})$ in eq. (2.2) and describes the sweeping interaction. This is exactly the vertex which "survived" in the infrared asymptotic behavior of the divergent integrals corresponding to the sweeping interaction. We shall call it the *sweeping* vertex. In expression (6.4), the contribution of the sweeping interaction to the full and sweeping vertices is precisely compensated in the marker point \mathbf{r}_0 . As a result, in this point W describes only the dynamic interaction. It would be natural to call this vertex the *dynamic* vertex.

We give some asymptotic expressions for the vertices T and W when one group of wave vectors $\boldsymbol{\kappa}$ and $\boldsymbol{\kappa}_1$ is much smaller than another group \mathbf{k} and \mathbf{k}_1 :

$$T(\mathbf{k}, \boldsymbol{\kappa}; \mathbf{k}_1, \mathbf{k}_2) \sim \boldsymbol{\kappa} \cdot \mathbf{k} \delta(\mathbf{k} - \mathbf{k}_1 - \mathbf{k}_2), \quad (6.5a)$$

$$T(\boldsymbol{\kappa}, \boldsymbol{\kappa}_1; \mathbf{k}, \mathbf{k}_1) \sim \boldsymbol{\kappa} \cdot \boldsymbol{\kappa}_1 \delta(\mathbf{k} + \mathbf{k}_1), \quad (6.5b)$$

$$T(\boldsymbol{\kappa}, \mathbf{k}; \boldsymbol{\kappa}_1, \mathbf{k}_1) \sim \mathbf{k} \min(\boldsymbol{\kappa}, \boldsymbol{\kappa}_1) \delta(\mathbf{k} - \mathbf{k}_1), \quad (6.5c)$$

$$\begin{aligned} W(\boldsymbol{\kappa}, \mathbf{k}_1; \mathbf{k}_2, \mathbf{k}_3) &\sim \boldsymbol{\kappa} \cdot \{ (\boldsymbol{\psi}_{13} [\delta(\mathbf{k}_1 - \mathbf{k}_2 - \mathbf{k}_3) - \delta(\mathbf{k}_1 - \mathbf{k}_3)]) \\ &\quad + \boldsymbol{\psi}_{12} [\delta(\mathbf{k}_1 - \mathbf{k}_2 - \mathbf{k}_3) - \delta(\mathbf{k}_1 - \mathbf{k}_2)] \} \sim \boldsymbol{\kappa} \mathbf{k}, \end{aligned} \quad (6.6a)$$

$$W(\boldsymbol{\kappa}, \boldsymbol{\kappa}_1; \mathbf{k}, \mathbf{k}_1) \sim \kappa \kappa_1 \delta(\mathbf{k} + \mathbf{k}_1), \quad (6.6b)$$

$$W(\boldsymbol{\kappa}, \mathbf{k}; \boldsymbol{\kappa}_1, \mathbf{k}_1) \sim (\kappa \kappa_1) (\kappa_j - \kappa_{1j}) \delta'_j(\mathbf{k} - \mathbf{k}_1) + [\boldsymbol{\kappa} \cdot \boldsymbol{\kappa}_1 - (\mathbf{k} \cdot \boldsymbol{\kappa})(\mathbf{k} \cdot \boldsymbol{\kappa}_1)/k^2] \delta(\mathbf{k} - \mathbf{k}') \sim \kappa \kappa_1. \quad (6.6c)$$

Here $\delta'_j(\mathbf{k}) = \partial \delta(\mathbf{k}) / \partial k_j$, $j = x, y, z$ is the vector index. The asymptotic form (6.6c) of the dynamic vertex W is (κ/k) times as small as the asymptotic form (6.5a) of the full vertex T . The smallness of W in this region reflects the locality of the dynamic interaction. This difference in asymptotic behavior will be sufficient to prove diagram convergence in the quasi-Lagrangian approach. Another fact that radically discriminates the dynamic vertex $W(\mathbf{k}_0; \mathbf{k}_1, \mathbf{k}_2; \mathbf{k}_3, \mathbf{k}_4)$ from the full one $T(\mathbf{k}_1, \mathbf{k}_2; \mathbf{k}_3, \mathbf{k}_4)$ is that it does not contain the factor $\delta(\mathbf{k}_1 + \mathbf{k}_2 - \mathbf{k}_3 - \mathbf{k}_4)$ proportional to the T vertex. Of course, nonpreservation of wave vectors in the W vertex is a result of the loss of spatial uniformity of the theory in the variables b and b^* due to the presence of the marker point \mathbf{r}_0 in the change of variables (6.2).

6.3. On the diagrammatic perturbation theory for b and b^*

To describe the turbulence arising in a flow around a certain body, for example, a lattice, one should solve the Navier–Stokes equations with given boundary conditions. Instead of this very complex problem, Wyld suggested [25] that an infinite volume of fluid at rest (on average) should be considered in which turbulence is excited by a random force introduced into the right-hand side of the Navier–Stokes equations as a model. In order to make such a formulation agree with the physics of the problem, one should assume that the pair correlation function of this force is well localized in the energy-containing interval: its \mathbf{k} -Fourier transform should diminish so rapidly for $k > 1/L$ and $\omega > V_T/L$ that it may be neglected in the inertial interval. In accordance with the hypothesis about the universal character of small-scale turbulence, we suppose that in the range $kL \rightarrow \infty$ its statistical properties are independent of the statistics of the exciting force ψ . The latter may for convenience be regarded to be a Gaussian force. For technical reasons we introduce into the right-hand side of the equations a regular term f . By iterating the Navier–Stokes equations with respect to ψ , one can represent the fluid velocity v and the response $\delta v / \delta f$ (as $f \rightarrow 0$) as a power series of the interaction vertex and the random force ψ . Then one can construct a series for $\delta v / \delta f$ and vv^* , average over the Gaussian ensemble and derive a series for the averaged response to an infinitely small regular force f , the Green function $G = \langle \delta v / \delta f \rangle$, eq. (I.17), and for the pair correlation function of the velocity $F = \langle vv^* \rangle$, eq. (I.18). Each term of a series of this formal perturbation theory may be juxtaposed, following certain rules, to a diagram. This results in Wyld's diagram technique (DT) for the Navier–Stokes equations, which served and will serve as a mathematical apparatus for the modern statistical theory of turbulence.

The formulation of the diagram technique following Wyld for the canonical Clebsch variables a and a^* has been suggested by Zakharov and myself in ref. [62]. In section 10 such a diagram technique for the canonical variables in the quasi-Lagrangian approach [for the variables $b(\mathbf{r}_0, \mathbf{k}, t_0, \omega)$ and $b^*(\mathbf{r}_0, \mathbf{k}, t_0, \omega)$] will be formulated. It may be called the *canonical quasi-Lagrangian* DT. It is radically different from the DT for the Clebsch variables [62] (the *canonical* DT) in the following respects. As we have already mentioned, in eqs. (6.3) for b and b^* spatial uniformity has been lost. This is formally expressed by the above-mentioned loss of momentum in the vertex W , eq. (6.4). As a result, the objects of the canonical quasi-Lagrangian DT, the Green function $G(\mathbf{r}_0, \mathbf{k}_1, \mathbf{k}_2, \omega)$ and the pair correlation function $N(\mathbf{r}_0, \mathbf{k}_1, \mathbf{k}_2, \omega)$ of the variables b and b^* become nondiagonal in the momentum [i.e., not proportional to $\delta(\mathbf{k}_1 - \mathbf{k}_2)$], see formulae (10.1)]. Recall that the same nondiagonality is

characteristic for the corresponding functions G and F of the quasi-Lagrangian velocity u , see formulae (3.1), (3.2).

To prevent misunderstanding, it should be emphasized once more that, contrary to the statements made in ref. [64], nondiagonality of the functions G and N in $(\mathbf{k}_1 - \mathbf{k}_2)$ is a formal consequence of the fact that in the quasi-Lagrangian formulation of the theory (and, of course, in the equivalent procedure of “zero mode subtraction”), the marker point \mathbf{r}_0 has been explicitly specified. The nondiagonality of the theory in $(\mathbf{k}_1 - \mathbf{k}_2)$ has nothing to do with physical problems such as strong spatial fluctuations of the rate of energy dissipation, intermittency, etc. This nondiagonality is the price of eliminating the sweeping interaction in a limited region surrounding the marker point \mathbf{r}_0 .

6.4. *What is the consequence of the nondiagonality of the theory in the momenta?*

The answer is: it leads to enormous technical difficulties. It can be demonstrated first of all with reference to the Dyson equation for the Green function. In the canonical DT [62] this equation has the standard (for theoretical physics) form

$$G(\mathbf{k}, \omega) = G_0(\mathbf{k}, \omega)[1 + \Sigma(\mathbf{k}, \omega)G(\mathbf{k}, \omega)], \quad G_0(\mathbf{k}, \omega) = (\omega + i0)^{-1}. \quad (6.7)$$

Here G_0 is the Green function of a noninteracting field with zero quadratic Hamiltonian H_2 , the mass operator $\Sigma(\mathbf{k}, \omega)$ is the sum of compact (irreducible) diagrams of a certain form [see eq. (10.5)]. Equation (6.7) is formally algebraic and is solved trivially,

$$G(\mathbf{k}, \omega) = [\omega - \Sigma(\mathbf{k}, \omega) + i0]^{-1}. \quad (6.8)$$

In the momentum-nondiagonal canonical quasi-Lagrangian DT, the Dyson equation becomes an integral equation,

$$G(\mathbf{r}_0, \mathbf{k}_1, \mathbf{k}_2, \omega) = G_0(\mathbf{k}, \omega) \left(\delta(\mathbf{k}_1 - \mathbf{k}_2) + \int \Sigma(\mathbf{r}_0, \mathbf{k}_1, \mathbf{k}_3, \omega) G(\mathbf{r}_0, \mathbf{k}_3, \mathbf{k}_2, \omega) d\mathbf{k}_3 \right). \quad (6.9)$$

Therefore in this diagram technique it is impossible to obtain a direct expression for the Green function via the mass operator similar to (6.8).

Another difficulty involves the substantial complication of the analytical expressions for the diagrams representing mass operators. To illustrate this we shall consider one of the simplest expressions representing diagram 3 in the series (10.5) for $\Sigma_2(\mathbf{r}_0, \mathbf{k}_1, \mathbf{k}_2, \omega)$,

$$\begin{aligned} \Sigma_2(\mathbf{r}_0, \mathbf{k}_1, \mathbf{k}_2, \omega) = & \int d\mathbf{k}_3 d\mathbf{k}_4 d\mathbf{k}_5 d\mathbf{k}_6 d\mathbf{k}_7 d\mathbf{k}_8 d\omega_3 d\omega_4 d\omega_5 T_{15,34} T_{67,82} G(\mathbf{r}_0, \mathbf{k}_6, \omega_3) \\ & \times N(\mathbf{r}_0, \mathbf{k}_4, \mathbf{k}_7, \omega_4) N(\mathbf{r}_0, \mathbf{k}_8, \mathbf{k}_5, \omega_5) \delta(\omega + \omega_5 - \omega_3 - \omega_4). \end{aligned} \quad (6.10)$$

In the momentum-diagonal canonical DT, three of the six three-dimensional integrations (for example, over $d\mathbf{k}_6 d\mathbf{k}_7 d\mathbf{k}_8$) in the respective expressions are performed with the help of the δ -functions in the expressions

$$G(\mathbf{k}_1, \mathbf{k}_2, \omega) = G(\mathbf{k}_1, \omega) \delta(\mathbf{k}_1 - \mathbf{k}_2), \quad N(\mathbf{k}_1, \mathbf{k}_2, \omega) = N(\mathbf{k}_1, \omega) \delta(\mathbf{k}_1 - \mathbf{k}_2). \quad (6.11)$$

The fourth three-dimensional integration over dk_5 may be performed using the δ -function in the expression for the vertex $T_{12,34}$ substituting in the diagonal DT in expression (6.10) the dynamic vertex W . A further drastic simplification in the analysis of expressions similar to (6.10) in the diagonal diagram technique is achieved due to the fact that we know in advance the type of dependence of $G(\mathbf{k}, \omega)$ and $N(\mathbf{k}, \omega)$ on k . For isotropic turbulence in the inertial interval, it follows from scale invariance considerations that

$$G(k, \omega) = \frac{1}{ak^x} g(\omega/ak^x), \quad N(k, \omega) = \frac{b}{ak^{x+y}} n(\omega/ak^x). \quad (6.12)$$

Here a and b are dimensional factors, and g and n are nondimensional structural functions of the nondimensional argument $z = \omega/ak^x$. As a result, in the diagonal DT it is possible to examine the convergence of all integrals over wave vectors depending on the scaling indices x and y .

In the nondiagonal DT, the case is different. The scale invariance determines only the type of dependence on $\mathbf{k} = (\mathbf{k}_1 + \mathbf{k}_2)/2$, leaving the dependence on $s = \mathbf{k}_1 - \mathbf{k}_2$ indeterminate,

$$G(\mathbf{r}_0, \mathbf{k}_1, \mathbf{k}_2, \omega) = \frac{1}{as^3k^x} g(s \cdot \mathbf{r}_0, s/k, \omega/ak^x), \quad N(\mathbf{r}_0, \mathbf{k}_1, \mathbf{k}_2, \omega) = \frac{b}{as^3k^{x+y}} n(s \cdot \mathbf{r}_0, s/k, \omega/ak^x). \quad (6.13)$$

Therefore analysis of the convergence of integrals over wave vectors is impossible without answering the question how these functions behave as $s \rightarrow 0$ and as $s \rightarrow \infty$. Certainly, to analyse the convergence of integrals over frequencies, one should know the asymptotic behavior of the functions (6.13) as $\omega \rightarrow 0$ and $\omega \rightarrow \infty$. Thus the price of eliminating the sweeping interaction, nondiagonality of the theory in the momentum, is very high. However, detailed analysis (partially given in ref. [60]) shows that it is impossible to eliminate sweeping to all orders of perturbation theory in terms of the momentum-diagonal DT. Therefore, to solve the problem of eliminating the sweeping interaction in order obtain further progress in the theory of developed turbulence using a DT, one should pay this price in full.

7. A scheme to prove the hypothesis of locality of the dynamic interaction of eddies

At this point it is worthwhile to ask credit of the reader and examine this problem first in terms of the *quasi-classical approximation* suggested by Belinicher and myself in refs. [60, 38].

7.1. Quasi-classical approximation

In this approximation it is suggested that on all the internal diagram lines of the quasi-Lagrangian DT, the dependence of the functions $G(\mathbf{r} - \mathbf{r}_0, \mathbf{k}, \omega)$ and $N(\mathbf{r} - \mathbf{r}_0, \mathbf{k}, \omega)$ on \mathbf{r}_0 should be ignored by taking them in the point $\mathbf{r} = \mathbf{r}_0$ where sweeping has been completely eliminated. In conformity with the hypothesis of locality of the interaction in \mathbf{r} -space, the main contribution to the description of the dynamics of a k -eddy with its center in point \mathbf{r}_0 should be made by certain integrals of the functions G and N in the region $|\mathbf{r} - \mathbf{r}_0| < l(k) \approx 1/k$. In the quasi-classical situation studying the interaction of two groups of eddies of essentially different scales ($k_1 \ll k_2$), corrections to the quasi-classical approximation are small in the parameter $k_2/k_1 \ll 1$. Indeed, in this situation the dependence of $G(\mathbf{r}, \mathbf{k}_1, \omega_1)$ and $N(\mathbf{r}, \mathbf{k}_1, \omega_1)$ on \mathbf{r} is determined by the distortion of k_1 -eddies in the nonuniform part of the velocity field

of the k_2 -eddy. These functions change substantially if $r \simeq 1/k_2$. Therefore in the region we are considering, $r < 1/k$, the difference between these functions and their values in the point $r_0 = 0$ is small in the above parameter. But in fully developed turbulence, where motions of all scales are present at once, the quasi-classical approximation is uncontrollable. In a fortunate situation it may involve a numerically small parameter. In general it should give a qualitatively true description of turbulence.

The quasi-classical approximation substantially simplifies the formal apparatus of the theory, removing the most essential difficulties which are due to the nondiagonality of the DT in k . Indeed, in the k -representation the quasi-classical approximation means the following replacement of functions:

$$\begin{aligned} G(r_0, k_1, k_2, \omega) &\rightarrow G_\ell[(k_1 + k_2)/2, \omega] \delta(k_1 - k_2), \\ N(r_0, k_1, k_2, \omega) &\rightarrow N_\ell[(k_1 + k_2)/2, \omega] \delta(k_1 - k_2), \end{aligned} \quad (7.1a)$$

where the *local* functions G_ℓ and N_ℓ are associated with the initial functions G and N through a relation which follows from (3.3) if one puts $r = r_0$,

$$\psi_\ell(k, \omega) = \int \psi(r_0, k + s/2, k - s/2, \omega) \exp(is \cdot r_0) ds. \quad (7.1b)$$

Here ψ is either of the functions G or N . In the quasi-classical approximation, the diagonality in the wave vector is restored by force by using formulas (7.1). As a result, the number of arguments in the functions G_ℓ and N_ℓ and the number of integrations in the diagrams is the same as in the usual canonical DT for the Clebsch variables.

7.2. How to prove the IR and UV convergence of all integrals in diagrams of any order at least in the quasi-classical approximation

A full answer to this question is given in section 11. Here we only outline a scheme of an attempt to prove this. First of all, the requirement of scale invariance of the theory in the limit $kL \rightarrow \infty$ will allow us to determine the type of dependence of G_ℓ and N_ℓ on k ,

$$G_\ell(k, \omega) = \frac{1}{ak^x} g_\ell(\omega/ak^x), \quad N_\ell = \frac{b}{ak^{x+y}} n_\ell(\omega/ak^x), \quad (7.2)$$

which coincide with the form of eqs. (6.12). An efficient analysis of integrals in the diagrams is impossible due to the lack of information on the type of functions $g_\ell(\xi)$ and $n_\ell(\xi)$. Therefore we make one more assumption (which will be proved later), that the integrals over ξ of these functions converge. This allows us to integrate in a general form over all ω_j of the internal lines and this reduces the four-dimensional DT (with integrations over $d^3k_j, d\omega_j$ on every closed contour) to a three-dimensional form (with integration over d^3k_j). In this case every diagram of the three-dimensional DT differs from the respective diagram of the four-dimensional DT by a limited factor. In the three-dimensional reduction of the DT, the functions $G_\ell(k)$ and $N_\ell(k)$ have a simple form,

$$G_\ell(k) = G_\ell(k, 0) = 1/ak^x, \quad N_\ell(k) = \int N_\ell(k, \omega) d\omega = b/k^y. \quad (7.3)$$

Thus all integrals in every diagram are given explicitly. This allows one to analyse, without spending much effort, any diagram for convergence (from infinite series for G and N). Considering these diagrams closely, we single out in subsection 11.3 the ways to integrate the most dangerous ones in the infrared region ($k_j \ll k$, k is the external wave vector) and prove the convergence in the IR region. In subsection 11.4 we single out from the integration cycles the most dangerous ones in the ultraviolet region. These proofs are based on the fact that the dynamic vertex $W(r_0, k_1, k_2; k_3, k_4)$ of the theory is essentially smaller than the full vertex $T(k_1, k_2; k_3, k_4)$ in the asymptotic region where $k_2, k_3 \ll k_1$ or $k_2, k_4 \ll k_1$.

7.3. A scheme to prove convergence of integrals in the quasi-Lagrangian nondiagonal diagram technique

The quasi-classical approximation considered in section 7.1 gives a qualitatively correct picture of developed turbulence but it naturally cannot claim to give a quantitative description because the functions $G(r_0, k_1, k_2, \omega)$ and $N(r_0, k_1, k_2, \omega)$ are not local in the difference $s = k_1 - k_2$ in the region $s \ll k = |k_1 + k_2|/2$. In reality, these functions should be expected to be local in s in the region $s \approx k$, since in the case of integral convergence there is no other parameter with the dimension of momentum in the theory.

As already mentioned, the main difficulty in the analysis of integral convergence in the quasi-Lagrangian DT nondiagonal in k is the absence of information on the type of dependence of the objects of the theory G and N on s and ω . We shall avoid it in the same way as in the quasi-classical approximation we avoided the problem of the dependence of G_ℓ and N_ℓ on ω . Namely, we first suggest that these dependences are such that the integrals over s and ω converge. Then one can integrate in general form over all ω_j and s_j of internal lines and thus reduce the seven-dimensional DT (with integrations over $d^3s_j d^3k_j d\omega_j$ on every closed contour) to a three-dimensional form (with integration over d^3k_j). After that the problem of proving integral convergence is reduced to the one solved in sections 7.2 and 11.

It is now necessary to pay off the credit and prove integral convergence in s and ω in the theory. For this we shall have to find the asymptotic behavior of G and N .

8. Asymptotic behavior of the Green function G and the pair correlation function N in s and ω

The schemes to find the asymptotic behavior of the functions G and N in different limits differ essentially. They will be described in sections 12–14. Here we only give and discuss results (for the scaling indices $x = 2/3$ and $y = 13/3$ corresponding to the Kolmogorov–Obukhov picture of turbulence).

8.1. Asymptotic behavior of the functions $G(r - r_0, k, \omega)$ and $N(r - r_0, k, \omega)$ in the mixed r, k representation

We shall see below that for $|r - r_0| \ll 1/k$, the functions G and N are continuous in r , i.e., the limit $r \rightarrow r_0$ exists. In this limit

$$G(0, k, \omega) = G_\ell(k, \omega) = \frac{1}{\Omega(0, k)} g_\ell(\omega/\Omega(0, k)), \quad (8.1a)$$

$$N(0, \mathbf{k}, \omega) = N_\ell(\mathbf{k}, \omega) = \frac{N(\mathbf{k})}{\Omega(0, \mathbf{k})} f_\ell(\omega/\Omega(0, \mathbf{k})), \quad (8.1b)$$

$$\Omega(0, \mathbf{k}) = a_0 k^{2/3} = (\varepsilon/\rho)^{1/3} k^{2/3}. \quad (8.1c)$$

Here $N(\mathbf{k})$ is the one-time correlation function of the quasi-Lagrangian variables b, b^* , coinciding, as mentioned in section 3, with the one-time correlation function of the Clebsch variables a, a^* . The function $f_\ell(z)$ should be normalized in such a way that $\int f_\ell(z) dz = 1$. In the inertial interval ($k \gg 1/L$)

$$N(\mathbf{k}) = b/k^{13/3}.$$

For $\omega \gg \Omega(0, \mathbf{k})$ we obtain for the local structure functions g_ℓ and f_ℓ in section 14 the following asymptotic forms:

$$g_\ell = \Omega(0, \mathbf{k})/\omega + ic_\ell [\Omega(0, \mathbf{k})/\omega]^4, \quad f_\ell = d_\ell [\Omega(0, \mathbf{k})/\omega]^{21/2}, \quad \Omega(0, \mathbf{k}) = a_0 k^{2/3}. \quad (8.2)$$

Here a_ℓ, c_ℓ and d_ℓ are unknown dimensionless factors. For $\omega < ak^{2/3}$, the functions g_ℓ and f_ℓ are regular, i.e., the dimensionless quantities $g_\ell(0)$ and $f_\ell(0)$ are finite and seem to be of the order of unity. It is seen from (8.2) that f_ℓ decreases as $\omega \rightarrow \infty$ rapidly enough so that the integral of f_ℓ over ω converges. This proves locality of the dynamic interaction in t and finishes the proof of locality in \mathbf{k} in the quasi-classical approximation.

Let us consider now the behavior of the functions G and N for $|\mathbf{r} - \mathbf{r}_0| \gg 1/k$. In this case, one can single out a most significant diagram sequence describing the sweeping interaction, discarding the diagrams describing the dynamic interaction, which are $(k|\mathbf{r} - \mathbf{r}_0|)^{1/3}$ times as small. In section 12 this sequence is summed. As a result, we get

$$G(\mathbf{r} - \mathbf{r}_0, \mathbf{k}, \omega) = \langle (\omega - \mathbf{k} \cdot \delta V + i0)^{-1} \rangle, \quad N(\mathbf{r} - \mathbf{r}_0, \mathbf{k}, \omega) = N(\mathbf{k}) \langle \delta(\omega - \mathbf{k} \cdot \delta V) \rangle, \quad (8.3a, b, c)$$

$$\delta V = \mathbf{v}(\mathbf{r}, t) - \mathbf{v}(\mathbf{r}_0, t).$$

Let us explain the physical sense of these expressions. By changing to quasi-Lagrangian variables, we have excluded the sweeping in the marker point \mathbf{r}_0 . At $\mathbf{r} \neq \mathbf{r}_0$, the compensation of sweeping is incomplete. In the region we are considering, $L \gg |\mathbf{r} - \mathbf{r}_0| = l$, the main contribution to the residual velocity of sweeping $\delta V(l)$ is made by the eddies of scale l . For $l > 1/k$, the Doppler frequency of sweeping $kV(l) = \omega_D(1/l, k)$, eq. (1.2), is much greater than the dynamic interaction frequency of k -eddies $\gamma(\mathbf{k})$, which is estimated by formula (1.3a). In a reference system moving with the k -eddies and in the absence of their dynamic interaction, the functions G and N should coincide with the functions G_0 and N_0 for a noninteracting field,

$$G(\mathbf{r} - \mathbf{r}_0, \mathbf{k}, \omega) \rightarrow G_0(\mathbf{k}, \omega) = (\omega + i0)^{-1}, \quad N(\mathbf{r} - \mathbf{r}_0, \mathbf{k}, \omega) \rightarrow N_0(\mathbf{k}, \omega) = N(\mathbf{k})\delta(\omega). \quad (8.4)$$

In a laboratory reference system (where the fluid is at rest on average), the frequency ω acquires the Doppler term $\mathbf{k} \cdot \mathbf{V}(\mathbf{r}, t)$ and formulas (8.4) change to formulas similar to (1.4). In a reference system moving at a rate $\mathbf{V}(\mathbf{r}, t)$, the Doppler shift is $\mathbf{k} \cdot \delta V$ [the difference δV has been determined in (8.3) and formulas (8.4) obviously are changed to (8.3)].

We have already remarked that in the region $L \gg |\mathbf{r} - \mathbf{r}_0| = l$, the chief contribution to δV is made by the $1/l$ -eddies whose characteristic velocity (2.3) is estimated by (2.4). Therefore averaging in (8.3) gives

$$G(\mathbf{r}, \mathbf{k}, \omega) = \frac{1}{\Omega(\mathbf{r}, \mathbf{k})} g_s(\omega/\Omega(\mathbf{r}, \mathbf{k})), \quad N(\mathbf{r}, \mathbf{k}, \omega) = \frac{N(k)}{\Omega(\mathbf{r}, \mathbf{k})} n_s(\omega/\Omega(\mathbf{r}, \mathbf{k})). \quad (8.5a)$$

Here $\Omega(\mathbf{r}, \mathbf{k}) = k \delta v(r)$ is the characteristic Doppler frequency of the sweeping of k -eddies in the velocity field $\delta v(r)$ of $1/r$ -eddies defined in eq. (2.4),

$$\Omega(\mathbf{r}, \mathbf{k}) = a_2 k r^{1/3} \simeq k(\varepsilon r/\rho)^{1/3}, \quad (8.5b)$$

for $L \gg r \gg 1/k$. Formulas (8.3) are evidently also true in the region $|\mathbf{r} - \mathbf{r}_0| \gg L$, when the distance between the points \mathbf{r} and \mathbf{r}_0 is significantly larger than the scale of the largest energy-containing vortices. In this region the velocities $\mathbf{v}(\mathbf{r}, t)$ and $\mathbf{v}(\mathbf{r}_0, t)$ are statistically independent. Therefore expressions (8.3) for G and N simplify to the form

$$G(\mathbf{r} - \mathbf{r}_0, \mathbf{k}, \omega) = G(\infty, \mathbf{k}, \omega) = \langle [\omega - \mathbf{k} \cdot (\mathbf{V}_a - \mathbf{V}_b) + i0] \rangle, \quad (8.6a)$$

$$N(\mathbf{r} - \mathbf{r}_0, \mathbf{k}, \omega) = N(\infty, \mathbf{k}, \omega) = N(k) \langle \delta(\omega - \mathbf{k} \cdot (\mathbf{V}_a - \mathbf{V}_b)) \rangle. \quad (8.6b)$$

Here the velocities \mathbf{V}_a and \mathbf{V}_b are statistically independent and have the same correlation,

$$\langle \mathbf{V}_a^m \mathbf{V}_b^n \rangle = \langle \mathbf{V}_a^m \rangle \langle \mathbf{V}_b^n \rangle, \quad \langle \mathbf{V}_{a,b}^n \rangle = \langle [\mathbf{V}(\mathbf{r}, t)]^n \rangle. \quad (8.6c)$$

The averaging procedure for (8.6) leads to formulas similar to (8.5),

$$G(\infty, \mathbf{k}, \omega) = \frac{1}{\Omega(\infty, \mathbf{k})} g_\infty(\omega/\Omega(\infty, \mathbf{k})), \quad N(\infty, \mathbf{k}, \omega) = \frac{N(k)}{\Omega(\infty, \mathbf{k})} n_\infty(\omega/\Omega(\infty)), \quad (8.7a, b)$$

$$\Omega(\infty, \mathbf{k}) = a_3 k L^{1/3} \simeq k(\varepsilon L/\rho)^{1/3} \simeq k V_T. \quad (8.7c)$$

It should be stressed that, in spite of the outer similarity of formulas (8.1), (8.5) and (8.7) specifying the behavior of the functions G and N in the regions $r \ll 1/k$, $L \gg r \gg 1/k$ and $r \gg L$, respectively, the physics of the processes in these regions is different. Therefore the functions g_ℓ , g_s and g_∞ , as well as f_ℓ , f_s and f_∞ do not coincide with each other.

8.2. Asymptotic behavior of the functions $G(\mathbf{k} + \mathbf{s}/2, \mathbf{k} - \mathbf{s}/2, \omega)$ and $N(\mathbf{k} + \mathbf{s}/2, \mathbf{k} - \mathbf{s}/2, \omega)$ in the \mathbf{s}, \mathbf{k} representation

Let us represent the unknown functions G and N as

$$G(\mathbf{k} + \mathbf{s}/2, \mathbf{k} - \mathbf{s}/2, \omega) = G_1(\mathbf{k}, \omega) \delta(\mathbf{s}) + G_2(\mathbf{s}, \mathbf{k}, \omega), \quad (8.8)$$

$$N(\mathbf{k} + \mathbf{s}/2, \mathbf{k} - \mathbf{s}/2, \omega) = N_1(\mathbf{k}, \omega) \delta(\mathbf{s}) + N_2(\mathbf{s}, \mathbf{k}, \omega).$$

Here the functions G_2 and N_2 are either regular as $s \rightarrow 0$ or have in this region an integrable singularity. We first of all note that for $r \gg l$, the functions $G(r, k, \omega)$ and $N(r, k, \omega)$ become constant as $r \rightarrow \infty$, eq. (8.7). Therefore, in the s -representation we have terms proportional to $\delta(s)$. From (7.1) we get

$$G_1(k, \omega) = G(\infty, k, \omega), \quad N_1(k, \omega) = N(\infty, k, \omega). \quad (8.9)$$

It should be noted that the results obtained here for the part of G and N that is diagonal in s radically differ from the analogous results obtained in ref. [64]. Its authors state that G_1 and N_1 have the Kolmogorov scaling index not only in the one-time pair correlation function but also in the frequency. Their resulting equations have the form, in our notation,

$$G_1(k, \omega) = \frac{1}{ak^{2/3}} g(\omega/ak^{2/3}), \quad N_1(k, \omega) = \frac{N(k)}{ak^{2/3}} n(\omega/ak^{2/3}). \quad (8.10)$$

Technically, the difference between solutions (8.10) and (8.7), (8.9) is reduced to the question of the IR convergence of the integrals of these functions. As the problem of IR convergence of integrals is radically important for the theory of turbulence, in section 13.1 I shall give another derivation of formulas (8.7), (8.9) following the scheme of derivation used by the authors of ref. [64] and indicate the place where they have made a mistake.

Let us proceed with our discussion of formulas (8.8). The behavior of the functions G_2 and N_2 in s in the region $s \ll k$ is determined by the functions $G(r, k, \omega)$ and $N(r, k, \omega)$, eq. (8.5), in the region $1/r \ll k$. This gives

$$G_2(s, k, \omega) = \frac{1}{a_2 k s^{8/3}} g_2(\omega s^{1/3}/a_2 k), \quad N_2(s, k, \omega) = \frac{N(k)}{a_2 k s^{8/3}} n_2(\omega s^{1/3}/a_2 k). \quad (8.11)$$

The asymptotic behavior of the functions G and N for $s \gg k$ is determined in section 12 from the analysis of diagrams in the s -representation. The result has the form

$$G_2(s, k, \omega) = \frac{1}{a_3 s^{11/3}} g_3(\omega/a_3 s^{2/3}), \quad N_2(s, k, \omega) = \frac{b}{a_3 s^8} n_3(\omega/a_3 s^{2/3}). \quad (8.12)$$

Using formulas (8.12), one can determine the law according to which the functions $G(r, k, \omega)$ and $N(r, k, \omega)$ tend to their limiting values (8.1) as $r \rightarrow 0$.

It is most essential for us that as $s \rightarrow \infty$ the functions G_2 and N_2 decrease more rapidly than $1/s^3$ according to eqs. (8.12). This provides convergence of the integrals of G_2 and N_2 over s in the UV region. It is also very important that as $s \rightarrow 0$, these functions increase more slowly than $1/s^3$ according to eqs. (8.11). This ensures the convergence of the above integrals also in the IR region. These two factors together provide the existence of the functions $G(r, k, \omega)$ and $N(r, k, \omega)$ as $r \rightarrow 0$ and afford a proof of the locality of the dynamic interaction of k -eddies in k -space. The full convergence of integrals over s leads to the fact that the main contribution to integrals over s_j on the internal lines in the diagrams is made by the region $s_j \approx k_j$. This will allow us to determine in section 14 the asymptotic behavior of the functions G_2 and N_2 for $\omega \gg ak^{3/2}$,

$$G_2(s, k, \omega) = \frac{\varphi_a}{k^{11/3}} \left(\frac{a_4 k^{2/3}}{\omega} \right)^{17/2}, \quad N_2(s, k, \omega) = \frac{b\varphi_b}{k^8} \left(\frac{a_4 k^{2/3}}{\omega} \right)^{15}. \quad (8.13a, b)$$

Here φ_a and φ_b are second-order polynomials in $s \cdot k/k^2$. It is extremely important for us that the functions G_2 and N_2 decrease rapidly enough as $\omega \rightarrow \infty$ to provide convergence of integrals of them over ω and to prove locality of the dynamic interaction of eddies in time. Together with locality in r (provided by the convergence in s), this allows us to finish the complete proof of the convergence of integrals in ω , s and k in the quasi-Lagrangian theory and thus to prove Kolmogorov–Obukhov scaling.

9. Kolmogorov–Obukhov scaling and the asymptotic form of multipoint correlation functions

9.1. Scaling relation

Let us consider the Dyson equation (6.9) in the quasi-Lagrangian canonical DT, substituting, e.g., expression (6.10) for Σ . We shall take the functions G and N in the scale invariant form (6.13). Due to convergence of all integrals, the main contribution in the integrations over s and k on the internal lines will be made by the region $s_j \simeq k_j \simeq k$ (here k is the external wave vector), and in the integration over ω_j by the region $ak_j^{2/3}$. This allows us to establish the following relation for the indices x and y :

$$x + y = t + d = 5, \quad (9.1)$$

where $W \sim k^t$, $t = 2$ is the scaling index of the W vertex, $d = 3$ is the dimension of space. Condition (9.1) is called the scaling relation. This relation has been obtained in ref. [62] in the canonical DT for the Clebsch variables, under the assumption that all integrals over k_j and ω_j converge. The assumption of convergence is incorrect for the Clebsch variables a^* and a : the sweeping interaction leads to IR divergence of the integrals over k . As a result, instead of (9.1), one has the relation $x = 1$, y is arbitrary. In the quasi-Lagrangian variables b and b^* , however, the sweeping has been eliminated, all integrals converge and the scaling relation (9.1) is true.

It is important to note that the scaling relation (9.1) guarantees that in the scale invariant solution (6.13), diagrams with any number of vertices will have the same order of magnitude. This follows from the convergence of the integrals and from the fact that addition of one eddy $W \sim k^t$ to the diagram leads to the addition of one Green function $G \sim 1/k^x s^d$, one pair correlation function $N \sim 1/k^{x+y} s^d$, two integrations $d^d s_j$, one integration over ω_j , and one integration $d^d k_j$. Estimating integrals over ω_j as ak^x , integrals over $d^d s_j$ and $d^d k_j$ as k^d , we see that the diagrams with n and $n + 1$ W vertices differ by a factor

$$WGNk^{3d+x} \simeq k^{t+d-x-y},$$

which, by (9.1) has zero scale dimension (i.e., is proportional to k^0) and is generally of the order of unity.

9.2. Dynamic relation for the scaling indices

This relation,

$$y = 13/3, \quad (9.2)$$

has also been established by Zakharov and me in ref. [62] for the canonical DT under the assumption that all integrals converge. It is much more hidden in diagram series than the scaling relation (9.1) lying

on the surface. We shall not summarize here the derivation of the dynamic relation (9.1) for the case of quasi-Lagrangian variables, though this is possible. In order to establish this relation in the quasi-Lagrangian DT, we shall make use of the fact that it is equivalent to the condition of constancy of the energy flux in the spectrum $\varepsilon(k)$, i.e., the condition that the scale dimension of this quantity is equal to zero: $\varepsilon(k) \simeq k^l$, $l=0$. The quantity l may be related to the scale dimension z_3 of the one-time triple velocity correlation function, $F^{(3)}(\mathbf{k}_1, \mathbf{k}_2, \mathbf{k}_3) \sim k^{-z_3}$. To do this let us write the Euler equation (I.2) for an incompressible fluid in the \mathbf{k}, t representation,

$$\frac{\partial v_i(\mathbf{k}, t)}{\partial t} = \frac{1}{2} \int \Gamma_{ijl}(\mathbf{k}, \mathbf{k}_1, \mathbf{k}_2) v_j(\mathbf{k}_1, t) v_l(\mathbf{k}_2, t) \delta(\mathbf{k} - \mathbf{k}_1 - \mathbf{k}_2) d\mathbf{k}_1 d\mathbf{k}_2, \quad (9.3)$$

where the Euler vertex Γ is a homogeneous function of first order in the k_j ,

$$\Gamma_{ijl}(\gamma \mathbf{k}, \gamma \mathbf{k}_1, \gamma \mathbf{k}_2) = \gamma \Gamma_{ijl}(\mathbf{k}, \mathbf{k}_1, \mathbf{k}_2).$$

In the case of homogeneous turbulence it follows from (9.3) that

$$\frac{\partial F_{ij}(\mathbf{k}, t)}{\partial t} = \frac{1}{2} \text{Im} \int \Gamma_{ilm}(\mathbf{k}, \mathbf{k}_1, \mathbf{k}_2) F_{lmj}^{(3)}(\mathbf{k}, \mathbf{k}_1, \mathbf{k}_2, t) \delta(\mathbf{k} - \mathbf{k}_1 - \mathbf{k}_2) d\mathbf{k}_1 d\mathbf{k}_2, \quad (9.4a)$$

where $F_{ij} = F_{ij}^{(2)}(\mathbf{k}, t)$ and $F_{ijl}^{(3)}(\mathbf{k}, \mathbf{k}_1, \mathbf{k}_2, t)$ are the double and triple velocity correlation functions in the \mathbf{k}, t representation. Equation (9.4a) describes the evolution of the energy spectrum. Due to conservation of the total energy of turbulence in the Euler equation, eq. (9.4a) may be written in a divergent form. In the isotropic case

$$\partial E(\mathbf{k}, t) / \partial t + (\partial / \partial k) \varepsilon(\mathbf{k}, t) = 0, \quad (9.4b)$$

where $E(\mathbf{k}, t)$ is the energy spectrum (I.7) and $\varepsilon(\mathbf{k}, t)$ is the energy flux in \mathbf{k} -space, which may be expressed via $F^{(3)}$ with the help of eq. (9.4a) [2]. Here we do not give this expression. It is only important for us that

$$\varepsilon(k) \sim k^{d+1} \Gamma(k) F^{(3)}(k, k, k), \quad (9.5a)$$

where $d=3$ is the dimension of space. It follows from (9.5a) that

$$l = 7 - z_3. \quad (9.5b)$$

The connection of the scale dimension z_3 of $F^{(3)}$ with the scaling indices x and y may be established from the first diagram for $F^{(3)}$ under the assumption that all integrals converge and the scaling relation (9.1), guaranteeing coincidence of the scale dimension of all higher-order diagrams with that of the first diagram, is satisfied. Expressing the Euler velocity by formula (5.5) in terms of the Clebsch variables a and a^* , and then a, a^* by formula (6.2a) in terms of b, b^* , we get

$$F^{(3)}(\mathbf{k}_1, \mathbf{k}_2, \mathbf{k}_3) = \int \varphi_{45} \varphi_{67} \varphi_{89} N^{(6)}(\mathbf{k}_4, \mathbf{k}_6, \mathbf{k}_8; \mathbf{k}_5, \mathbf{k}_7, \mathbf{k}_9) \\ \times \delta(\mathbf{k}_1 + \mathbf{k}_4 - \mathbf{k}_5) \delta(\mathbf{k}_2 + \mathbf{k}_6 - \mathbf{k}_7) \delta(\mathbf{k}_3 + \mathbf{k}_8 - \mathbf{k}_9) d\mathbf{k}_4 \cdots d\mathbf{k}_9. \quad (9.6a)$$

Here $N^{(6)}$ is the one-time correlation function of the sixth-order quasi-Lagrangian variables b and b^* (coinciding with that for the Clebsch variables a and a^*). The scale dimension of $N^{(6)}$ may be found by calculating $N^{(6)}$, for example, in the Gaussian approximation (i.e., in the zeroth order in the interaction),

$$N^{(6)}(\mathbf{k}_4, \mathbf{k}_6, \mathbf{k}_8; \mathbf{k}_5, \mathbf{k}_7, \mathbf{k}_9) = N(\mathbf{k}_4)N(\mathbf{k}_6)N(\mathbf{k}_8)\delta(\mathbf{k}_4 - \mathbf{k}_9)\delta(\mathbf{k}_6 - \mathbf{k}_5) + \dots$$

Substituting this expression into (9.6a) we have

$$F^{(3)}(\mathbf{k}_1, \mathbf{k}_2, \mathbf{k}_3) = \int \varphi(\mathbf{k}_4, \mathbf{k}_1 + \mathbf{k}_4)\varphi(\mathbf{k}_1 + \mathbf{k}_4, \mathbf{k}_1 + \mathbf{k}_2 + \mathbf{k}_4)\varphi(\mathbf{k}_4 - \mathbf{k}_3, \mathbf{k}_4) \\ \times N(\mathbf{k}_4)N(\mathbf{k}_1 + \mathbf{k}_4)N(\mathbf{k}_4 - \mathbf{k}_3) d\mathbf{k}_4 + \dots \quad (9.6b)$$

Substituting here $N(t) \approx k^{-y}$ and taking into account the convergence of the integral over k , we have for $k_1 \approx k_2 \approx k_3 \approx k$

$$F^{(3)}(k) \approx k^{6-3y}.$$

Together with expression (9.5b) this gives $l = 13 - 3y$. Since $l = 0$, $y = 13/3$. This is just the dynamic relation (9.2) obtained earlier for the Clebsch variables.

Substituting $y = 13/3$ into the scaling relation (9.1), we find $x = 2/3$. This implies that the frequency of the dynamic interaction of eddies $\gamma(k) \approx k^{2/3}$ by formula (I.10c) obtained from the dimensional analysis in the Richardson–Kolmogorov–Obukhov theory of turbulence.

Let us now find the scale dimension z of the one-time pair correlation function of the Euler velocity, $F(k) \approx k^{-z}$. One can obtain an expression for $F(k)$ similar to eq. (9.6b),

$$F(k) = \int |\varphi(\mathbf{k}_1, \mathbf{k} + \mathbf{k}_1)|^2 N(\mathbf{k}_1)N(\mathbf{k} + \mathbf{k}_1) d\mathbf{k}_1 + \dots \quad (9.7)$$

This gives the relation

$$z = 2y - 5 \quad (9.8)$$

between the scale dimensions of the one-time pair correlation functions of the Euler velocity (z) and of the canonical variables a, a^* or b, b^* (y). Formulas (9.2) and (9.8) yield

$$z = 11/3. \quad (9.9)$$

From this, for the spectrum of turbulence $E(k)$, the Kolmogorov–Obukhov “five-thirds law” (I.9) follows. Thus, the solution of the diagram equations which we have obtained describes the known Richardson–Kolmogorov–Obukhov picture of turbulence. This is not surprising since they follow from dimensional considerations under the assumption that the energy-containing scale L_{ext} and viscous scale L_{int} of turbulence do not enter the theory of the dynamic interaction of eddies because of its locality. Are the values of the Kolmogorov index $x = 2/3$ and $y = 13/3$ established finally? Is the Richardson–Kolmogorov–Obukhov picture of turbulence realized in reality? What are we to do with intermittency? Some considerations regarding these extremely important issues will be given in the conclusion.

9.3. Multipoint one-time velocity correlation functions

We note once more that a dimensional analysis allows one to establish in the Richardson–Kolmogorov–Obukhov picture of turbulence the k -dependence of the dynamic interaction frequency $\gamma(k) \sim k^{2/3}$ and the velocity pair correlation function $F(k) \approx k^{-11/3}$. For higher-order velocity correlation functions, only the general scale dimension z_n may be determined from a dimensional analysis, while their dependence on the dimensionless wave vector correlation functions remains unknown,

$$F^{(3)}(\mathbf{k}_1, \mathbf{k}_2, \mathbf{k}_3) = k_1^{-z_3} f_3(\mathbf{k}_2/k_1, \mathbf{k}_3/k_1), \quad (9.10a)$$

$$F^{(4)}(\mathbf{k}_1, \mathbf{k}_2, \mathbf{k}_3, \mathbf{k}_4) = k_1^{-z_4} f_4(\mathbf{k}_2/k_1, \mathbf{k}_3/k_1, \mathbf{k}_4/k_1), \quad \dots, \quad (9.10b)$$

$$F^{(n)}(\mathbf{k}_1, \dots, \mathbf{k}_n) = k_1^{-z_n} f_n(\mathbf{k}_2/k_1, \dots, \mathbf{k}_n/k_1), \quad (9.10c)$$

$$z_2 = z = 11/3, \quad z_3 = 7, \quad z_4 = 31/3, \quad \dots, \quad z_n = 10n/3 - 3. \quad (9.10d)$$

The theory developed here allows a determination of the asymptotic behavior of the functions f_n when one of the wave vectors or the sum of a group of wave vectors is small compared to the others.

Let us first consider the triple correlation function $F^{(3)}(\mathbf{k}_1, \mathbf{k}_2, \mathbf{k}_3)$ in the region where $k_1 = \kappa \ll k_2 \approx k_3 \approx k$. In this case, the main contribution to the integral (9.6b) is made by the region $k \approx \kappa$. This gives

$$F^{(3)}(\kappa, \mathbf{k}, \mathbf{k}) \approx \kappa^{-8/3} k^{-13/3} \varphi_3(\kappa/k). \quad (9.11)$$

The function φ_3 depends only on the direction of κ and is odd under the transformation $\kappa \rightarrow -\kappa$. Expression (9.6b) naturally represents only one term of an infinite formal diagram series for $F^{(3)}$ where all terms are of the same order of magnitude due to the scaling relation (9.1). One can show that the asymptotic behavior (9.11) may be reproduced in the quasi-Lagrangian DT in each term of this series. The diagrams of the DT for the Clebsch variables have no such property. Thus, *the asymptotic behavior of multipoint velocity correlation functions may be studied on the first diagrams only in the quasi-Lagrangian DT.*

We shall now consider the analytical expression for the first term of a diagram series for $F^{(4)}$. It may be derived similarly to eqs. (9.7) and (9.6) for $F^{(2)}$ and $F^{(3)}$ by expressing the Euler velocity according to formula (5.5) in the Clebsch variables a and a^* , and then a and a^* in b and b^* according to formula (6.2), and, finally, by splitting the eighth-order correlation function of the variables b and b^* into products of pair correlation functions. This gives

$$\begin{aligned} F^{(4)}(\mathbf{k}_1, \mathbf{k}_2, \mathbf{k}_3, \mathbf{k}_4) = & \int \varphi(\mathbf{k}_5, \mathbf{k}_5 + \mathbf{k}_1) \varphi(\mathbf{k}_5 + \mathbf{k}_1, \mathbf{k}_5 + \mathbf{k}_1 + \mathbf{k}_2) \varphi(\mathbf{k}_5 + \mathbf{k}_1 + \mathbf{k}_2, \mathbf{k}_5 - \mathbf{k}_3) \varphi(\mathbf{k}_5 - \mathbf{k}_3, \mathbf{k}_5) \\ & \times N(\mathbf{k}_5) N(\mathbf{k}_5 + \mathbf{k}_1) N(\mathbf{k}_5 + \mathbf{k}_1 + \mathbf{k}_2) N(\mathbf{k}_5 - \mathbf{k}_4) d\mathbf{k}_5 + \dots \end{aligned} \quad (9.12)$$

If any of the wave vectors (for example, $k_1 = \kappa$) is much smaller than the others, the main contribution to the integral (9.12) is made by the region $k_5 \approx \kappa$ and

$$F(\kappa, \mathbf{k}_2, \dots) \sim \kappa^{-8/3}. \quad (9.13)$$

Here we have intentionally omitted the index $n = 4$, as this asymptotic form is valid for any n , not only for $n = 3$ [see eq. (9.11)] and for $n = 4$.

Now let $\boldsymbol{\kappa} = \mathbf{k}_1 + \mathbf{k}_2 = -(\mathbf{k}_3 + \mathbf{k}_4)$, $\kappa \ll k_1, k_3$. Then the main contribution to (9.12) will be made by the regions $k_5 \simeq \kappa$ and

$$F^{(4)}(\mathbf{k}_1, -\mathbf{k}_1 + \boldsymbol{\kappa}, \mathbf{k}_3, -\mathbf{k}_3 - \boldsymbol{\kappa}) \simeq \kappa^{-5/3} k_1^{-13/3} k_3^{-13/3}. \quad (9.14)$$

This asymptotic behavior is also reproduced in the essential sequence of higher-order diagrams.

In a similar way one can treat higher-order correlation functions $F^{(n+m)}$, where $m, n > 2$. If $\mathbf{k}_1 + \mathbf{k}_2 + \dots + \mathbf{k}_n = \boldsymbol{\kappa}$, $\kappa \ll k_j$, then

$$F^{(n+m)} \simeq \kappa^{5/3} k_1^{-(10n-7)/3} k_{n+1}^{-(10m-7)/3}. \quad (9.15)$$

Here we have assumed that all wave vectors of the first group are of the order of k_1 , those of the second group of the order of k_{n+1} .

In conclusion, I shall give without derivation the following *rule of splitting the irreducible velocity correlation functions*, which is inferred by prolonged contemplation of the diagram series and seems to be correct:

$$\begin{aligned} & F_{\alpha_1, \alpha_2, \dots, \alpha_n; \beta_1, \beta_2, \dots, \beta_m}^{(n+m)}(\mathbf{k}_1, \mathbf{k}_2, \dots, \mathbf{k}_n, \mathbf{k}_{n+1}, \dots, \mathbf{k}_{n+m}) \\ &= \left(\sum_{\gamma} F_{\alpha_1, \alpha_2, \dots, \alpha_n, \gamma}^{(n+1)}(\mathbf{k}_1, \mathbf{k}_2, \dots, \mathbf{k}_n, -\boldsymbol{\kappa}) F_{\gamma, \beta_1, \dots, \beta_m}^{(m+1)}(+\boldsymbol{\kappa}, \mathbf{k}_{n+1}, \dots, \mathbf{k}_{n+m}) \right) / \sum_{\gamma} F_{\gamma\gamma}^{(2)}(\boldsymbol{\kappa}). \end{aligned} \quad (9.16)$$

Here $n, m > 2$ and it is suggested that $\kappa = |\mathbf{k}_1 + \dots + \mathbf{k}_n| \ll k_j$, $j = 1, 2, \dots, n + m$. In the coordinate representation, this correlation function describes the law of damped correlations when a compact group of n points with characteristic distance $l_2 \simeq 1/k_1$ between them is at a large distance $R \simeq 1/\kappa$ from another group of m points with a mutual distance $l_2 \simeq 1/k_{n+1}$. It is easy to see that the correlation function (9.15) is a particular case of (9.16). The rule of splitting (9.16) will be derived in a future publication.

PART II: MATHEMATICAL APPARATUS OF THE THEORY

10. Diagram technique for the quasi-Lagrangian Clebsch variables b and b^*

Let us add to the right-hand side of eqs. (6.3) for $b(\mathbf{r}_0, \mathbf{k}, t_0, t)$, in conformity with Wyld's idea [25], a Gaussian random force $\varphi(\mathbf{r}_0, \mathbf{k}, t)$ simulating turbulence excitation and a vanishingly small regular force $f(\mathbf{r}_0, \mathbf{k}, t)$. By analyzing with formulas (3.1), (3.2), we shall define (in the \mathbf{k} -representation) the Green function G as the linear response of a turbulent field b to a force f and the pair correlation function N of this field,

$$G(\mathbf{r}_0, \mathbf{k}_1, \mathbf{k}_2, \omega_1) \delta(\omega_1 - \omega_2) = \langle \delta b(\mathbf{r}_0, \mathbf{k}_1, t_0, \omega_1) / \delta f(\mathbf{r}_0, \mathbf{k}_2, t_0, \omega_2) \rangle, \quad (10.1a)$$

$$N(\mathbf{r}_0, \mathbf{k}_1, \mathbf{k}_2, \omega_1) \delta(\omega_1 - \omega_2) = \langle b(\mathbf{r}_0, \mathbf{k}_1, t_0, \omega_1) b^*(\mathbf{r}_0, \mathbf{k}_2, t_0, \omega_2) \rangle. \quad (10.1b)$$

Here averaging is done over the Gaussian force ensemble φ . For the reasons we have already discussed, the functions G and N do not depend on t_0 , are diagonal in ω and nondiagonal in \mathbf{k} .

Now we can represent $b(\mathbf{r}_0, \mathbf{k}, t_0, \omega)$, using eq. (6.3), as an iteration series in powers of $WG_0^*G_0^2\varphi^*\varphi^2$. Here G_0 is the zero-order Green function of the equation. It is specified in formula (6.7). Then one can construct a series for $\delta b/\delta f$ and bb^* , average over the Gaussian ensemble and derive series for G and N . The Dyson summation of weakly linked (reducible) diagrams results in a system of Dyson, eq. (6.9), and Wyld equations,

$$N(\mathbf{r}_0, \mathbf{k}_1, \mathbf{k}_2, \omega) = \int d\mathbf{k}_3 d\mathbf{k}_4 G(\mathbf{r}_0, \mathbf{k}_1, \mathbf{k}_3, \omega) [D(\mathbf{r}_0, \mathbf{k}_3, \mathbf{k}_4, \omega) + \Phi(\mathbf{r}_0, \mathbf{k}_3, \mathbf{k}_4, \omega)] G_0^*(\mathbf{r}, \mathbf{k}_4, \mathbf{k}_2, \omega). \quad (10.2)$$

In these equations D is the pair correlation function of the random force φ . The mass operators Σ and Φ are sums of compact (irreducible) diagrams of a certain form. For their representation we introduce the following graphical symbols:

$$\begin{aligned} G(\mathbf{r}_0, \mathbf{k}_1, \mathbf{k}_2, \omega) &\sim \overset{1}{\text{---}} \overset{2}{\text{---}}, & G^*(\mathbf{r}_0, \mathbf{k}_1, \mathbf{k}_2, \omega) &\sim \overset{1}{\text{---}} \overset{2}{\text{---}}, \\ N(\mathbf{r}_0, \mathbf{k}_1, \mathbf{k}_2, \omega) &\sim \overset{1}{\text{---}} \overset{2}{\text{---}}, & N^*(\mathbf{r}_0, \mathbf{k}_1, \mathbf{k}_2, \omega) &= N(\mathbf{r}_0, \mathbf{k}_2, \mathbf{k}_1, \omega) \sim \overset{1}{\text{---}} \overset{2}{\text{---}}, \\ W(\mathbf{r}_0, \mathbf{k}_1, \mathbf{k}_2, \mathbf{k}_3, \mathbf{k}_4) &\sim \begin{array}{c} \text{---} \text{---} \text{---} \\ \diagup \quad \diagdown \\ \text{---} \quad \text{---} \\ \diagdown \quad \diagup \\ \text{---} \text{---} \end{array}, & W^*(\mathbf{r}_0, \mathbf{k}_1, \mathbf{k}_2, \mathbf{k}_3, \mathbf{k}_4) &\sim \begin{array}{c} \text{---} \text{---} \text{---} \\ \diagdown \quad \diagup \\ \text{---} \quad \text{---} \\ \diagup \quad \diagdown \\ \text{---} \text{---} \end{array}. \end{aligned} \quad (10.3)$$

These symbols are dictated by the functional approach [2, 38, 39, 65] to deriving Wyld's DT. They automatically specify all topological properties of the diagrams for the mass operators described in ref. [62]. In this notation the compact diagrams for Σ have one straight and one wavy end, those for Φ have two straight ends,

$$\begin{aligned} \Sigma(\mathbf{r}_0, \mathbf{k}_1, \mathbf{k}_2, \omega) &= \overset{1}{\text{---}} \text{---} \overset{2}{\text{---}}, & \Sigma^*(\mathbf{r}_0, \mathbf{k}_1, \mathbf{k}_2, \omega) &= \overset{1}{\text{---}} \text{---} \overset{2}{\text{---}}, \\ \Phi(\mathbf{r}_0, \mathbf{k}_1, \mathbf{k}_2, \omega) &= \Phi^*(\mathbf{r}_0, \mathbf{k}_1, \mathbf{k}_2, \omega) = \overset{1}{\text{---}} \text{---} \overset{2}{\text{---}}. \end{aligned} \quad (10.4)$$

We give the first diagrams for these operators,

$$\begin{aligned} \text{---} \text{---} \text{---} &= \text{---} \text{---} \text{---} + 1/2 \text{---} \text{---} \text{---} + \text{---} \text{---} \text{---} + \\ &+ \text{---} \text{---} \text{---} + \text{---} \text{---} \text{---} + \text{---} \text{---} \text{---} + \\ &+ \text{---} \text{---} \text{---} + \text{---} \text{---} \text{---} \end{aligned} \quad (10.5)$$

$$\begin{aligned}
 & \text{Diagram 1} = 1/2 \text{ Diagram 1} + \text{Diagram 2} + \dots \\
 & + \text{Diagram 3} + \text{Diagram 4} + \dots
 \end{aligned}
 \tag{10.6}$$

The rules for reading these diagrams are as usual. They may be recollected by comparing diagram 3 in the series (10.5) with its analytical expression (6.10).

11. Analysis of diagram convergence in the quasi-classical approximation

11.1. The Dyson–Wyld equations in the quasi-classical approximation

As we mentioned in section 7.1, the quasiclassical approximation implies that in all internal lines of diagrams, the functions $N(\mathbf{r}_0, \mathbf{k}_1, \mathbf{k}_2, \omega)$ and $G(\mathbf{r}_0, \mathbf{k}_1, \mathbf{k}_2, \omega)$ undergo forced diagonalization according to the rule (7.1). In order to have this approximation closed, we should derive the Dyson–Wyld equations for the local functions $G(\mathbf{k}, \omega)$ and $N(\mathbf{k}, \omega)$. They follow from the initial Dyson–Wyld equations (6.9) and (10.2) after their integration according to the rule (7.1b),

$$\begin{aligned}
 G_\ell(\mathbf{k}, \omega) &= G_0(\mathbf{k}, \omega) - \int G_\ell(\mathbf{k} + \mathbf{s}/2, \omega) \Sigma_\ell(\mathbf{k} + \mathbf{s}/2, \mathbf{k} - \mathbf{s}/2, \omega) G_\ell(\mathbf{k} - \mathbf{s}/2, \omega) ds, \\
 N_\ell(\mathbf{k}, \omega) &= \int G_\ell(\mathbf{k} + \mathbf{s}/2, \omega) \Phi_\ell(\mathbf{k} + \mathbf{s}/2, \omega) G_\ell^*(\mathbf{k} - \mathbf{s}/2, \omega) ds.
 \end{aligned}
 \tag{11.1}$$

Here Σ_ℓ and Φ_ℓ are the local mass operators; they are functionals of G and N . The expressions for them follow from the diagram expansions (10.5), (10.6) after the replacement in (7.1) has been made.

11.2. Reduction of the diagram technique to three-dimensional form

As usual, we shall seek a solution of the Dyson–Wyld equations (in the limit $kL \rightarrow \infty$) in the scale invariant form (7.2). Regarding the form of the structural functions we assume (and will prove later) that $n_\ell(z)$ is finite everywhere, decreasing rather rapidly as $z \rightarrow \infty$. $\text{Re}\{g_\ell(z)\}$ behaves in the same manner, while $\text{Im}\{g_\ell(z)\}$ is zero at $z = 0$ and behaves as $1/z$ for $z \rightarrow \infty$. Now we shall integrate over all internal frequencies in some diagram for the Green function (GF). The number of integrations is equal to that of various pair correlation functions (PC) in this diagram: $j = 1, \dots, n$. The GF frequencies $\tilde{\omega}_{n+1}, \dots, \tilde{\omega}_{2n+1}$ are linear combinations of the external frequency ω and the integration frequencies ω_j determined by the laws of frequency conservation in vertices. The three-momenta of all the lines (GF and PC) will be regarded as independent since the three-momentum is not conserved in a quasi-Lagrangian vertex (10.3), so it is unreasonable to separate the diagram fragments corresponding to certain momentum paths as a result of integration over n frequencies ω_j ; each PC will preserve the scaling factor k^{-y} , so each GF will have the corresponding factor k^{-x} and the whole diagram will have one common factor, which is a function of many variables,

$$\begin{aligned}
 Y(\omega/k^x, \mathbf{k}/k, \mathbf{k}_1/k, \dots, \mathbf{k}_{2n-1}/k) = & \int g_0(\tilde{\omega}_{n+1}/k_{n+1}^x) g_\ell(\tilde{\omega}_{n+2}/k_{n+2}^x) \cdots g_\ell(\tilde{\omega}_{2n+1}/k_{2n+1}^x) \\
 & \times n_\ell(\omega_1/k_1^x) \cdots n_\ell(\omega_n/k_n^x) k_1^{-x} \cdots k_n^{-x} d\omega_1 \cdots d\omega_n. \quad (11.2)
 \end{aligned}$$

Here ω, \mathbf{k} are the external variables of the diagram for the GF. The expression for y in the PC diagrams is a bit modified: the index 0 on the first GF vanishes and one of the GFs in the backbone is replaced by a PC. A very important statement is that about the regularity of the function Y : it is finite over the whole range of variation of its arguments and may be expanded in a series in them. This follows from its explicit form (11.2) and the assumed properties of the structural functions g_ℓ and n_ℓ ensuring the existence of the integral (11.2) for all values of its parameters. Hence, when analyzing the convergence of integrals over the three-momenta in the diagrams, we can replace it with a constant. Then our diagrams will contain only three-dimensional integrations over \mathbf{k}_j of the internal lines in the mass operators, with

$$G_1(k) = 1/ak^x, \quad N_1(k) = bk^{-y}, \quad (11.3)$$

where a and b are some dimensional constants.

11.3. Analysis of the IR convergence of three-dimensional diagrams

In this section we will consider the case when a diagram fragment contains a momentum κ which is much smaller than the external momentum k . Topologically, three cases are possible for the small momentum: (1) it starts in one vertex and terminates in another; (2) it completes a cycle; (3) it branches and covers some region of the diagram.

In the first case, the following versions of the small momentum are possible:

$$(11.4)$$

where the vertices in which the small momentum κ starts or terminates are underlined. Let us determine the IR convergence index of a fragment as follows: If $\kappa \ll k$, the expression for this fragment is proportional to κ . For $\kappa > 0$, the integral over κ in the IR region will converge. By making use of the asymptotic behavior of the dynamic vertex W , eq. (6.6), we obtain for the convergence indices σ of the fragments in (11.4)

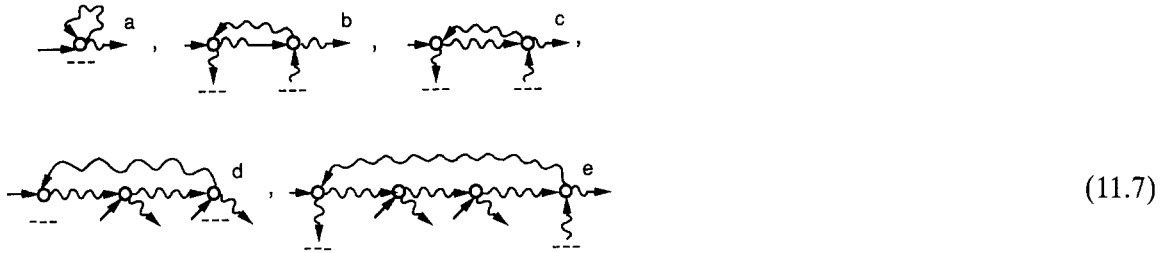
$$\sigma_a = \sigma_b = 5 - x, \quad \sigma_c = 5 - y = x, \quad \sigma_e = \sigma_f = 10 - 2y = 2x. \quad (11.5)$$

Here we have made use of the scaling relation of the canonical DT [62],

$$x + y = 5. \quad (11.6)$$

Since $1 > x > 0$, all σ in (11.5) are positive and all fragments in (11.4) converge. The lowest rate of convergence is shown by fragment c of (11.4) with one PC. Elongation of the small momentum line by one PC [compare fragments c, e and f, in (11.4)] leads to addition of a vertex $W \sim \kappa^2$, an integration over $d\kappa$ and a PC $N \sim \kappa^{-y}$, together a factor $\kappa^{5-y} = \kappa^{+x}$, which improves the IR convergence. The case is, however, different with the Euler canonical DT containing no subtraction of sweeping. The middle vertex T of fragment e is proportional to $k \cdot \kappa$, and the additional factor will reduce the rate of convergence from c to e, so that fragments with a large number of PCs in the Euler DT will diverge.

In the second case, the following versions of cyclic flow of the small momentum are of interest:

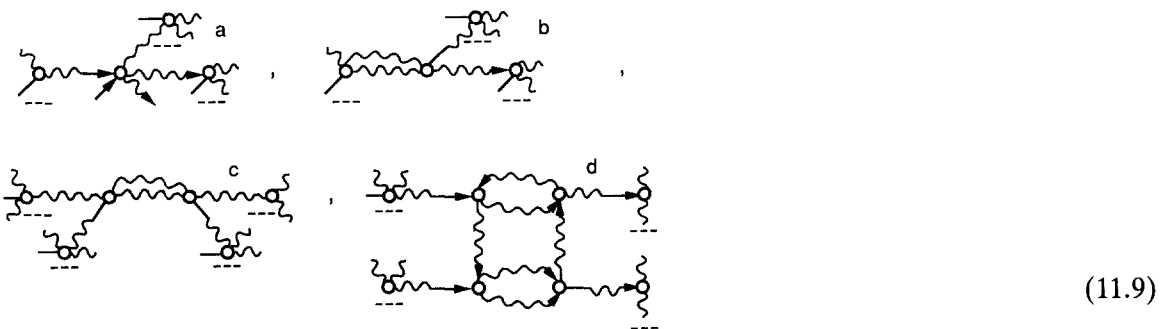


The convergence indices of these fragments are

$$\sigma_a = x, \quad \sigma_b = 5, \quad \sigma_c = 2x, \quad \sigma_d = 3x, \quad \sigma_e = 4x. \quad (11.8)$$

The smallest cycle a converges as κ^x . Comparison of fragments b and e shows that the smallest rate of convergence belongs to the PC. Increasing the length of the cycle by one PC improves convergence by κ^x , since it adds one PC $\sim \kappa^{-y}$, one vertex $W \sim \kappa^2$ and one integration over $d\kappa$. In the Euler DT the vertex $T \sim k \cdot \kappa$ and addition of a PC deteriorates convergence by κ^{x-1} , so that cycles with a PC will diverge for small κ [35].

In the third case, let us consider the following fragments of diagrams with small momenta:



The IR convergence indices then are

$$\sigma_a = \sigma_b = \sigma_c = \sigma_d = 2x > 0, \quad (11.10)$$

all being positive.

All these indices are negative. This ensures integral convergence of these fragments in the UV region. Comparison of the indices σ_c , σ_d and σ_e shows that increased cycle length with a PC increases the convergence rate.

A smaller rate of convergence should be expected in the $1, n$ cycles, consisting of one PC and n GFs,



$$(11.16)$$

For this fragment $\sigma_f = y - 2 - nx$, and the convergence rate grows with n . This is a property of the quasi-Lagrangian DT. In the Euler DT a different asymptotic behavior of a vertex T leads to the UV index $\tilde{\sigma}_f = x - 1 + n(1 - x)$, so that rather long $1, n$ cycles in the Euler DT are divergent.

In the third case, fragments (11.19), we have

$$\sigma_a = -2, \quad \sigma_b = \sigma_c = 2x - 7, \quad \sigma_d = 6x - 17. \quad (11.17)$$

Thus in all the cases considered here, the UV indices are negative, and the integrals in the corresponding diagram fragments converge. When the large momentum takes up a large inner part of the diagram the scaling relation begins to operate so that this large fragment converges.

Some worry is caused by the fact that small or large momenta may go out to the end of the diagram. For example, the diagram



$$(11.18)$$

logarithmically diverges in the UV region. Divergence of this sort is unique. Fortunately, one can prove the Ward identity, from which it follows that the diverging parts of these diagrams compensate each other. No UV divergences associated with diagram ends appear, since the large integration momentum p always takes up at least one PC.

Hence we have proved that IR and UV divergences are also absent when the Hamiltonian approach is applied to the quasi-classical approximation of fully developed hydrodynamic turbulence. Earlier, in ref. [38], Belinicher and the present author gave a similar proof based on the Euler equations for natural variables. Thus in the quasi-classical approximation, the interaction is local due to the scaling relation and energy conservation; the Dyson–Wyld diagram equations have the solutions (7.2) with Kolmogorov indices $x = 2/3$, $y = 13/3$.

12. Structural functions of the quasi-Lagrangian theory and locality of the interaction

12.1. Reduction of the canonical quasi-Lagrangian diagram technique to three-dimensional form

In the asymptotic limit $kL \rightarrow 0$, we will seek the solution of the Dyson–Wyld equations (6.9) and (10.2) in the scale invariant form (6.13). The reduction of the seven-dimensional quasi-Lagrangian DT to three-dimensional form is done in the same way as in the quasi-classical approximation. Namely, assuming convergence of the integration over ω , we carry out all integrations in the diagrams over ω_j of

the internal lines. As a result, they will have a regular function Z similar to the function Y , eq. (11.2),

$$Z(\omega/k^x, k/k, s/k, k_1/k, s_1/k, \dots, s_{2n-1}/k). \quad (12.1)$$

Then let us assume that integrals over s_j also converge and perform these integrations. In the integral over s_j , the main contribution is made by the region where s_j is of the order of its k_j . Therefore after integrations over all s the function Z goes over into the regular function Y , eq. (11.2), which is finite in the whole range of variation of its parameters and may be expanded in them. Due to this, it may be majorized with a constant, and the whole reasoning of section 11 on convergence of the integration over k may be repeated. The problem of momenta extending to the boundaries of a diagram does not arise, as in calculating the diagrams for $G(r_0, k + s/2, k - s/2, \omega)$ and $N(r_0, k + s/2, k - s/2, \omega)$ one does not have to integrate over the momentum s corresponding to the ends of a diagram.

Comparing the reduction of the two DT to three-dimensional form (the four-dimensional DT in the quasi-classical approximation and the seven-dimensional quasi-Lagrangian DT) one can say that in the former the functions $G(r - r_0, k, \omega)$ and $N(r - r_0, k, \omega)$ are replaced by their value in the marker point $r = r_0$, and in the latter by some mean value in the interaction region $k|r - r_0| < 1$, which is different for different diagrams.

Thus we have proved locality of the dynamic interaction of eddies in k -space (convergence of all integrals over k) by assuming this interaction to be local in r -space (integral convergence over s_j) and time (integral convergence over ω_j). Our next step will be investigating the asymptotic behavior of the functions G and N to make sure that the integrals of the theory over s_j and ω_j converge. At this stage we will assume the dynamic interaction to be entirely local (i.e., the integrals over k_j , s_j and ω_j converge). Let us begin with the simple case.

12.2. Asymptotic behavior of the Green function G and the pair correlation function N for $s \gg k$

In all the diagrams, the arguments of both the G and N lines and the W vertices contain the combinations $k \pm s/2$ corresponding to wave vectors of the entry (first) and exit (last) diagram lines. The value $k = 0$ in these arguments is not specified. Therefore the limit $k \rightarrow 0$ exists (and coincides with the value for $k = 0$) and in all arguments of the diagrams one may set $k = 0$. As a result, for $s \gg k$, the dependence of each diagram on k (and, consequently, the functions N and G) vanishes. It is necessary for this to happen that in the limit $s \gg k$, the structural functions g and n in formulas (6.13) (with the values of the Kolmogorov scaling indices $x = 2/3$, $y = 13/3$) should change to

$$g(k \cdot r_0, s/k, \omega/ak^{2/3}) \rightarrow k^{2/3} g(k \cdot r_0, \omega/as^{2/3}), \quad n(k \cdot r_0, s/k, \omega/ak^{2/3}) \rightarrow k^5 n(k \cdot r_0, \omega/as^{2/3}). \quad (12.2)$$

From this and from (6.9) formulas (8.10) for the asymptotic behavior of G and N for $s \gg k$ follow, which was given by eqs. (8.12).

12.3. Asymptotic behavior of the functions G and N for $L^{-1} \ll s \ll k$

This is found by a more complex argument. It is simplest to give it in the mixed k, r representation for $kr \gg 1$, and then pass over to the k, s representation. In section 8.1 we gave the physical

considerations establishing this asymptotic behavior. Here we will show how it is determined by diagram series. To this end we first remind the reader of some topological properties of mass operators (for details see, e.g., refs. [35, 62]):

(a) The diagrams have no closed loops from the Green functions.

(b) In diagrams for Σ , one can pass in only one way from the *entry* vertex (with a straight outer end) to the *exit* vertex (with a wavy end). In the diagram series (10.5), (10.6), the entry vertices are shown on the left, the exit ones on the right. This passage along the G_j and G_j^* lines is called the *backbone*. Apart from the functions G_j and G_j^* it includes also the vertices connecting them. Thus in diagram 1 in (10.5), the backbone consists of only one vertex, in diagrams 3, 4 and 5 it includes the function G and two vertices, in diagrams 2 and 6 the function G^* and two vertices, in diagram 7 two Green functions G_1 and G_2 and three vertices, etc.

(c) From any vertex not belonging to the backbone one can pass in only one way, along the Green functions, to the backbone. Such passages along G_j and G_j^* (including also the vertices linking them) are called *ribs*.

It should also be recalled that in the canonical DT the most IR-divergent sequence consists of diagrams where the backbone does not include the complex conjugate of the Green function. In the canonical quasi-Lagrangian DT, in the region $kr \ll 1$, the main contribution to the Green function will be made by the same sequence. Each dynamic W vertex in the backbone presents a difference between the full T vertex and two sweeping T vertices [see eq. (6.4a)]. If we introduce the following graphical symbols for the vertices T and T_s :

$$T(k_1, k_2, k_3, k_4) = \begin{array}{c} 2 \quad 3 \\ \diagup \quad \diagdown \\ \bullet \\ \diagdown \quad \diagup \\ 1 \quad 4 \end{array}, \quad T_s(r_0; k_1, k_2; k_3, k_4) = \begin{array}{c} 2 \quad 3 \\ \diagup \quad \diagdown \\ \bullet \\ \diagdown \quad \diagup \\ 1 \quad 4 \end{array}, \quad (12.3)$$

this difference may be represented in the form

$$W(r_0; k_1; k_2; k_3, k_4) = \begin{array}{c} 2 \quad 3 \\ \diagup \quad \diagdown \\ \circ \\ \diagdown \quad \diagup \\ 1 \quad 4 \end{array} = \begin{array}{c} 2 \quad 3 \\ \diagup \quad \diagdown \\ \bullet \\ \diagdown \quad \diagup \\ 1 \quad 4 \end{array} - \begin{array}{c} 2 \quad 3 \\ \diagup \quad \diagdown \\ \bullet \\ \diagdown \quad \diagup \\ 1 \quad 4 \end{array} - \begin{array}{c} 2 \quad 4 \\ \diagup \quad \diagdown \\ \bullet \\ \diagdown \quad \diagup \\ 1 \quad 3 \end{array} \quad (12.4)$$

Here we have located the lines 1 and 4, which we shall regard as belonging to the backbone, on one straight line.

One can make sure that for $kr \ll 1$ the diagrams containing the last term in (12.4) "cutting the backbone" are $(kr)^{-1/3}$ times as small as the main contribution. In this main contribution to the Green function, one can neglect the dependence of the backbone on the momenta k_1 and k_2 "attached" to it. Thus each Green function in the backbone has an external four-momentum k , ω as an argument and for $k_2, k_3 \ll k_1 \approx k_4$ every vertex (12.4) is given by

$$\begin{array}{c} 2 \quad 3 \\ \diagup \quad \diagdown \\ \circ \\ \diagdown \quad \diagup \\ 1 \quad 4 \end{array} \Rightarrow \begin{array}{c} 2 \quad 3 \\ \diagup \quad \diagdown \\ \bullet \\ \diagdown \quad \diagup \\ 1 \quad 4 \end{array} - \begin{array}{c} 2 \quad 3 \\ \diagup \quad \diagdown \\ \bullet \\ \diagdown \quad \diagup \\ 1 \quad 4 \end{array} \approx (k_1 \cdot \varphi_{23}) \{ \exp[i(k_2 - k_3) \cdot r] - \exp[i(k_2 - k_3) \cdot r_0] \}. \quad (12.5)$$

The exponential factor in the first diagram appeared in the transformation to the r representation by formula (3.3).

For the analysis of the resulting sequence of diagrams for the GF, the normal Dyson representation, in which weakly linked (irreducible) diagrams occur, is inconvenient. More adequate will be the “bare backbone” representation, in which the GFs of the backbone remain bare while the GFs of the ribs and all PCs are dressed. From the structure of this series it is clear that the sum of various many-tailed diagrams with a fixed number $2n$ of bonds at the backbone is the full (reducible) correlation function of the fields b and b^* ,

$$\begin{aligned} F(\mathbf{k}'_1, \omega'_1, \mathbf{k}''_1, \omega''_1, \mathbf{k}'_2, \omega'_2, \mathbf{k}''_2, \omega''_2, \dots, \mathbf{k}''_n, \omega''_n) \\ = \langle b(\mathbf{k}'_1, \omega'_1) b^*(\mathbf{k}''_1, \omega''_1) b(\mathbf{k}'_2, \omega'_2) b^*(\mathbf{k}''_2, \omega''_2) \cdots b^*(\mathbf{k}''_n, \omega''_n) \rangle. \end{aligned} \quad (12.6)$$

By each of the end pairs, \mathbf{k}'_j, ω'_j and $\mathbf{k}''_j, \omega''_j$, this correlation function is connected to the bare backbone through the vertex (12.5), and its integration over all $\mathbf{k}'_j, \omega'_j, \mathbf{k}''_j, \omega''_j$ is carried out by means of the weights (12.5). If we turn to the expression for the velocity in terms of the canonical variables a, a^* , eq. (6.1), taking into account that the simultaneous field correlations a and b (integrated over all frequencies) coincide, then it becomes apparent that integration (12.6) with the weights (12.5) yields

$$\langle \{ \mathbf{k} \cdot [\mathbf{v}(\mathbf{r}, t) - \mathbf{v}(\mathbf{r}_0, t)] \}^n \rangle.$$

This expression should be multiplied by $[G_0(\mathbf{k}, \omega)]^{n+1}$, $n+1$ being the number of bare GFs of the backbone, and summed over all n . The sum of this geometric progression gives the sought expression (8.3a) for the GF in the region $|\mathbf{r} - \mathbf{r}_0| \ll 1/k$.

As to the problem of finding the structure of the pair correlation function N , it is the same as in the case of the pair correlation function of the Euler velocity discussed in detail in refs. [38, 60]. Therefore we will not carry out a summation of the diagram series but restrict ourselves only to the qualitative physical considerations given in section 8.1 and leading to the solution (8.3b).

13. Direct calculation of the Green function and the pair correlation function diagonal in s

Following the authors of ref. [64], we shall seek a solution of the Dyson–Wyld integral equations (6.9) and (10.2) in the form (8.8). It may be easily seen that for the functions G_1 and N_1 there appear the usual equations not containing G_2 and N_2 ,

$$G_1(\mathbf{k}, \omega) = G_0(\mathbf{k}, \omega)[1 + \Sigma_1(\mathbf{k}, \omega)G_1(\mathbf{k}, \omega)], \quad N_1(\mathbf{k}, \omega) = G_1(\mathbf{k}, \omega)\Phi_1(\mathbf{k}, \omega)G_1^*(\mathbf{k}, \omega). \quad (13.1)$$

Here Σ_1 and Φ_1 are the parts of the mass operators Σ and Φ that are diagonal in s and are functionals of G_1 and N_1 . To obtain the expressions for Σ_1 and Φ_1 , let us substitute the graphical expression (12.4) for the dynamic vertex in the diagram expansion (10.5), (10.6). In first and second order of the interaction we have

(13.2a)

(13.2b)

Here we hold on to diagram numbering of the expansion (10.5): a diagram with number (m, n) is a term of the diagram with number m in (10.5). By direct substitution in (13.2a) of the diagram parts G_1 and N_1 diagonal in s [or proportional to $\delta(s)$], one can make sure that in nine diagrams (13.2a) the general momentum is preserved and their contribution to the mass operator Σ is diagonal in s , while all the remaining twelve diagrams do not possess these properties. It should be pointed out here that ref. [64] contains the statement, which is wrong in my opinion, that the diagrams 3.3 and 3.4 (and similar ones) are diagonal in the momentum [or proportional to $\delta(\mathbf{k} - \mathbf{k}')$ if all the lines of which they consist are also diagonal]. The proof given in ref. [64] is based on the representation

$$\delta(\mathbf{k} - \mathbf{k}' - \mathbf{k}'') = \exp(\mathbf{k}'' \cdot \partial / \partial \mathbf{k}) \delta(\mathbf{k} - \mathbf{k}'), \quad (13.3)$$

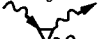
though it ignores the effect of the shift operator $\exp(\mathbf{k}'' \cdot \partial / \partial \mathbf{k})$ on the Green function which is to the right of the mass operator in the Dyson equation (6.7a). The entire proof [64] of integral convergence in the series for the parts of the GF and PC diagonal in s is based on the diagonality of diagrams of the type (13.2b). Thus we believe that this proof as well as the statement are wrong.

To analyze the form $G(\mathbf{k}, \omega)$ and $N(\mathbf{k}, \omega)$, we shall seek a solution of the Dyson–Wyld equation (13.1) in the scale invariant form

$$G_1(\mathbf{k}, \omega) = \frac{1}{ck^z} g_1(\omega/ck^z), \quad N_1(\mathbf{k}_1, \omega) = \frac{b}{ck^{y+z}} n_1(\omega/ck^z). \quad (13.4)$$

Here c and b are dimensional constants required for G and N to be dimensionless functions of dimensionless arguments. It has been shown in ref. [62] that in the absence of divergences in the integrals, the Dyson–Wyld diagram equations (13.1) have a solution corresponding to Kolmogorov’s concept of turbulence. It implies $z = 2/3$, $y = 13/3$. Divergences are, however, present, which leads to a rearrangement of the solution. We shall show that the diagram series for G_1 and N_1 of higher divergence may be summed very accurately.

By substituting G_1 and N_1 into the diagram series (13.2a) from (13.4) with the Kolmogorov index values ($z = 2/3$, $y = 13/3$), one can easily see that the greatest divergence in the region of small k is shown by two groups of diagrams for the PC. First, these are the diagrams $n.2$ ($n = 1, 3, 4, 5$) with kinematic vertices, and secondly, these are the diagrams $n.1$ ($n = 1, 3, 4, 5$) with the Euler vertices in the backbone oriented “in a normal way” . Diagram 2.1 in (13.2a) or similar ones contain vertices in the backbone with “anomalous” orientation , so they do not enter this series.

One can approximately calculate the integrals of the Euler diagram series $n.1$ ($n = 1, 3, 4, 5$) by making use of the fact that the main contribution to them is made by the domain in which the four-momenta of pair correlation functions are small compared to the external four-momenta running through the backbone. This permits one, first, to neglect all the momenta entering the backbone, that is, to consider all GFs of the backbone four-momenta to be equal to the external ones, and secondly, to use, instead of the exact expression of the Euler vertex $T(k_1, k_2; k_3, k_4)$, eq. (5.4b), its asymptotic value $T(k, \kappa; \kappa', k + \kappa - \kappa')$ for $\kappa, \kappa' \ll k$, coinciding with eq. (6.4) for the kinematic vertex when $r_0 = 0$. Graphically, this procedure corresponds to replacement of T_s in all Euler vertices of the backbone  in the series $n.1$ by the kinematic vertex .

The approximation described here is called the *sweeping approximation*, as mentioned in the foregoing discussion. It completely ignores the dynamic interaction of vertices. It is seen that the diagrams of the sweeping approximation in the $n.1$ and $n.2$ series with an even number of vertices on the backbone coincide, while those with an odd number have opposite signs. The diagrams with an odd number of vertices are simply zero in the case of the sweeping approximation, as they change sign after replacement of all integration variables $\kappa' \rightarrow -\kappa'$.

The diagram series ($n.1$) for the canonical variables was summed in ref. [35]. The summing procedure was described in detail in ref. [38] and was used here in section 12.3. Since the derived answer has a simple physical meaning which clearly raises no doubt, we shall write it down without repeating the derivation,

$$G_a(\omega, k) = G_s(\omega, k) = \langle (\omega + k \cdot V_a + i0)^{-1} \rangle. \quad (13.5a)$$

This expression coincides with eq. (1.4) and is the GF of noninteracting k -eddies, in which the Doppler frequency shift was taken into account because they are swept with velocity $v = V_a$ and which was averaged over an ensemble of turbulent velocities $v(r, t)$ at a fixed point and at one and the same moment of time,

$$\langle V_a^n \rangle = \langle [v(r, t)]^n \rangle. \quad (13.5b)$$

It may be easily understood now that summing the diagram series with sweeping vertices leads to the following expression for the GF:

$$G_b(\omega, k) = \langle (\omega + k \cdot V_b - i0)^{-1} \rangle, \quad (13.6a)$$

$$\langle V_b^n \rangle = \langle [\mathbf{v}(\mathbf{r}_0, t)]^n \rangle. \quad (13.6b)$$

This describes the sweeping of noninteracting eddies in the homogeneous velocity field $\mathbf{v} = -V_b$ with statistical properties (13.6b), which are the same as (13.5b).

Finally, consideration of both series (with full and sweeping vertices) and all interference diagrams (where both types of vertices occur) leads for G to our expressions (8.6a), (8.9). Likewise, for N one can again obtain our expressions (8.6b) and (8.9). As for the differing expressions (8.10) for G and N , which were obtained in ref. [64], they are erroneous for the reason stated above.

14. Calculation of the asymptotic behavior of the structural functions for large frequencies

In the proof of integral convergence in the quasi-classical and Lagrangian DTs, the rapid decrease of the structural functions $f(z), n(z)$ as $z \rightarrow \infty$, where $z = \omega/ak^{2/3}$, necessary for convergence of the integration over ω , was very important. Below we will establish the asymptotic behavior of the Green function and pair correlation function for $\omega \gg ak^{2/3}$. For this purpose we shall consider the local Green functions and the pair correlation functions which have the naive Kolmogorov scaling (7.2) with $x = 2/3, y = 13/3$. Let us find first the asymptotic behavior of the pair correlation function. To this end let us integrate the Wyld equation (10.2) over s and take the limit $\omega \rightarrow \infty$,

$$N(\mathbf{k}, \omega) = \int G(\mathbf{r}_0, \mathbf{k} + s/2, \mathbf{k}_1, \omega) \Phi(\mathbf{r}_0, \mathbf{k}_1, \mathbf{k}_2, \omega) G^*(\mathbf{r}_0, \mathbf{k}_2, \mathbf{k} - s/2, \omega) ds d\mathbf{k}_1 d\mathbf{k}_2. \quad (14.1)$$

One can make sure that as $\omega \rightarrow \infty$ the main contribution to the integrals in (14.1) is made by the integration domain over the internal frequencies $\omega_j \approx \omega$ and internal momenta $k_j \approx s_j \approx (\omega/a)^{3/2}$. The explicit form of the structural functions in G and N in the calculation of the integrals over the internal variables k_j, s_j and ω_j is inessential as $(\omega_j/a)^{3/2} \approx k_j \approx s_j$. Taking into account the general dimension of the functions G and N , eq. (6.11), the asymptotic behavior of the two "external" (in the Wyld equation) Green functions for $\omega \rightarrow \infty$,

$$G(\mathbf{k} + s/2, \mathbf{k} - s/2, \omega) \rightarrow \delta(s)/\omega,$$

and the proportionality of the mass operator to the square of the external wave vector \mathbf{k} , we get

$$\frac{1}{k^{15/3}} n_1(\omega/ak^{2/3}) \propto \frac{k^2}{k_j^{15/3}}, \quad k_j \approx (\omega/a)^{3/2}. \quad (14.2)$$

From this expression the asymptotic power law (8.2b) for the pair correlation function $N_\ell(\mathbf{k}, \omega)$ follows. Similar considerations may be applied to the Dyson equation, which has been integrated over s . This gives the asymptotic form (8.2a) for $G(\mathbf{k}, \omega)$ as $\omega \rightarrow \infty$. Both these asymptotic forms are easily verified by the first diagram for the mass operators Σ and Φ ; the scaling relation, in view of the power law in ω of the asymptotic forms (8.2) for G_ℓ and N_ℓ as $\omega \rightarrow \infty$, ensures reproduction throughout the whole diagram series.

On the basis of the same considerations regarding the dominant contribution of the integration domains $(\omega_j/a)^{3/2} \approx k_j \approx s_j \approx (\omega/a)^{3/2}$, regarding the proportionality of Σ and Φ to the square of the external wave vector \mathbf{k} and the asymptotic form $G \sim 1/\omega$ as $\omega \rightarrow \infty$, one can also find the asymptotic behavior for $(\omega/a) \gg k^{2/3}$ of the Green function and pair correlation function in the quasi-Lagrangian

theory; see formulas (8.13). These functions decrease rather rapidly with respect to ω , confirming the correctness of the conclusions about the regularity of the functions Y and Z , eqs. (11.2) and (12.1), introduced in proving diagram convergence.

15. Conclusion

Let us summarize the results of this work. At the current stage in the theory of fully developed uniform turbulence of an incompressible fluid, the major difficulties arising from the masking effect of the sweeping interaction are effectively solved by changing to a moving reference system associated with the fluid velocity in some reference point of space r_0 . This change of coordinates eliminates the sweeping of k -eddies in the region of scale $1/k$ surrounding the reference point r_0 . Elimination of sweeping in a limited region proves to be sufficient for the complete elimination from the theory of the masking effect of sweeping on the dynamic interaction of eddies in the cascade process of energy transfer to small scales.

The statistical theory of fully developed homogeneous turbulence of an incompressible fluid constructed in the present work is based on the Hamilton equations for an ideal fluid in the Clebsch variables and diagrammatic perturbation theory similar to Wyld's diagram technique for the Navier–Stokes equation. This theory is formulated in terms of the local Green function $G(r, k, \omega)$ and the local pair correlation function $N(r, k, \omega)$ describing the statistical properties of k -eddies in the vicinity of point r . These local functions replace in the new theory the global statistical characteristics $G(k, \omega)$ and $N(k, \omega)$, which in the traditional formulation of the theory of homogeneous uniform turbulence refer to the whole space.

This work analyses the analytical expressions for diagrams of arbitrary order in perturbation theory and shows that integrals converge both in the IR and UV regions. This proves the complete locality of the dynamic interaction of eddies: the main contribution to the changed energy of a k -eddy is made by other k_1 -eddies of the same scale (k_1 of the order of k) and located in a region of scale $1/k$ surrounding the given eddy.

In the limit $kL \rightarrow \infty$ (L is the energy-containing scale), a scale invariant solution of the Dyson–Wyld diagram equations has been obtained, which is consistent with the known Richardson–Kolmogorov–Obukhov concept of fully developed uniform turbulence.

This new theory provides techniques for calculating the statistical characteristics of turbulence. This application of the theory is a separate large and difficult research program, which is to be implemented in future. Here I have found for illustration the asymptotic behavior of simultaneous many-point velocity correlation functions when one of the wave vectors or the sum of a group of wave vectors tends to zero.

Previously, similar results have been obtained in the paper by Belinicher and myself [38], where the sweeping interaction was eliminated in a similar way and Wyld's diagrammatic perturbation theory was also used, but as the starting equations the Navier–Stokes equations were used. Thus, the statement [64] that the Hamiltonian approach produces a different picture of turbulence is incorrect and based on an obvious mistake. It has been found that the nonlinear change of variables $v \propto \varphi aa^*$ does not lead to essential modifications in the current structure of the theory. Neither can we ascertain the ultimate equivalence of these approaches. Some characteristics are more conveniently analyzed using the Clebsch variables, and others by means of the Euler velocity. Probably the next stage in the development of the theory will reveal more significant differences between these approaches.

It should be noted that the mathematical objects of the theory are asymptotic series depending on

external parameters. After the sweeping effects have been eliminated, they do not contain small alphabetic parameters. It is clear that partial summations of such series, which we have regularly performed, is a poorly defined mathematical procedure. Our quasi-Lagrangian diagram technique in terms of the dressed pair correlation functions, the Green function and the bare vertex functions may be regarded as a method of defining the original Euler diagram technique. This method provides physically meaningful results, giving us hope that the approximations of several first diagrams as well as the methods of asymptotic summation of the series, e.g. following Borel, will turn out to be sufficient for obtaining quantitative results. The problem of unambiguous correspondence of the observed physical quantities to asymptotic series of the theory of fully developed hydrodynamic turbulence is still open to discussion.

Nonperturbative contributions to fully developed turbulence are also possible (yielding zero in a series expansion in perturbation theory). We also note that in our solutions of the diagram equations, the vertex homogeneity index (scale dimension) is not renormalized. However, the theory may also contain some different solutions, in which the scale dimension of the vertex varies, but because of the scaling relation and locality of the interaction, the dimensions of the simultaneous velocity correlation functions remain unchanged.

A number of important problems remain uninvestigated, such as the uniqueness of the solution obtained, its stability and establishment, the transition of the nonuniversal solution in the energy interval to the scale invariant solution in the inertial interval, etc. Thus there is ample opportunity for further activities in this field.

In these studies, the method of the renormalization group (employed in the theory of turbulence in refs. [39–55]) should be extensively used for the analysis of diagram equations of the scale invariant theory of turbulence in the quasi-Lagrangian approach, where the sweeping has been eliminated and there are no integral divergences.

Acknowledgments

It is a pleasure to thank Prof. R. Kraichnan for useful discussions of the problem of eliminating sweeping. Special thanks are due to Victor Belinicher for numerous conversations on the problems of strong turbulence. This work has been supported by the Meyerhoff Foundation of the Weizmann Institute of Science, Rehovot, Israel.

References

- [1] L.D. Landau and E.M. Lifshitz, *Fluid Mechanics* (Nauka, Moscow, 1986) (in Russian) [English translation of 1954 edition publ. by Pergamon, Oxford (1959)].
- [2] A.S. Monin and A.M. Yaglom, *Statistical Fluid Mechanics* (Nauka, Moscow, 1967) (in Russian) [English translation publ. by MIT Press, Cambridge, MA (Vol. 1 1971, Vol. 2 1975)].
- [3] L.F. Richardson, *Weather Prediction by Numerical Process* (Cambridge Univ. Press, Cambridge, England, 1922) p. 66.
- [4] A.N. Kolmogorov, *Dokl. Akad. Nauk SSSR* 30 (1941) 299; 32 (1941) 19.
- [5] A.M. Obukhov, *Dokl. Akad. Nauk SSSR* 32 (1941) 22; *Izv. Akad. Nauk SSSR Ser. Geogr. Geofiz.* 5 (1941) 443.
- [6] L. Onsager, *Phys. Rev.* 68 (1945) 286.
- [7] W. Heisenberg, *Z. Phys.* 124 (1948) 628.
- [8] C.F. von Weizsäcker, *Z. Phys.* 124 (1948) 614.
- [9] H.L. Grant, R.W. Steward and A. Moilliet, *J. Fluid Mech.* 12 (1962) 241.
- [10] G.K. Batchelor and A.A. Townsend, *Proc. R. Soc. A* 199 (1949) 238.
- [11] A.Y. Kuo and S. Corrsin, *J. Fluid Mech.* 50 (1971) 285.

- [12] A.Y. Kuo and S. Corrsin, *J. Fluid Mech.* 56 (1972) 447.
- [13] A.N. Kolmogorov, *J. Fluid Mech.* 13 (1962) 82.
- [14] A.M. Obukhov, *J. Fluid Mech.* 12 (1962) 77.
- [15] E.A. Novikov and R.M. Stewart, *Izv. Akad. Nauk SSSR Ser. Geofiz.* 3 (1964) 408.
- [16] A.M. Yaglom, *Dokl. Akad. Nauk SSSR* 166 (1966) 49.
- [17] B.B. Mandelbrot, *J. Fluid Mech.* 62 (1974) 331.
- [18] B.B. Mandelbrot, in: *Turbulence and Navier–Stokes Equation*, ed. R. Teman, *Lecture Notes in Mathematics*, vol. 565 (Springer, Berlin, 1976) p. 121.
- [19] U. Frisch, P.L. Sulem and M. Nelkin, *J. Fluid Mech.* 87 (1978) 719.
- [20] M.D. Millionshchikov, *Dokl. Akad. Nauk SSSR* 32 (1941) 611.
- [21] M.D. Millionshchikov, *Izv. Akad. Nauk SSSR Ser. Geofiz.* 5 (1941) 433.
- [22] R.H. Kraichnan, in: *Proc. Symp. Dynamics of Fluids and Plasmas* (Academic Press, New York, 1967).
- [23] A.V. Shutko, *Dokl. Akad. Nauk SSSR* 158 (1964) 1058.
- [24] R.H. Kraichnan, *J. Fluid Mech.* 6 (1959) 497.
- [25] H.W. Wyld, *Ann. Phys.* 14 (1961) 143.
- [26] E.M. Lifshitz and L.P. Pitaevsky, *Physical Kinetics* (Pergamon, Oxford, 1981).
- [27] G.A. Kuzmin and A.Z. Patashinsky, *Zh. Eksp. Teor. Fiz.* 62 (1972) 1175.
- [28] B.B. Kadomtsev, in: *Voprosy Teorii Plazmy*, vol. 4, ed. M.A. Leontovich (Atomizdat, Moscow, 1964) [English translation: *Plasma Turbulence* (Academic Press, London, 1965)].
- [29] R.H. Kraichnan, *Phys. Fluids* 8 (1965) 575–598; 9 (1966) 1728.
- [30] G.A. Kuz'min and A.Z. Patashinskii, *Zh. Prikl. Mat. Tekh. Fiz.* 19 (1978) 62 [*J. Appl. Mech. Tech. Phys.* 19 (1978) 50].
- [31] T. Nakano and F. Tanaka, *Prog. Theor. Phys.* 65 (1981) 120.
- [32] S.S. Moiseev, A.V. Tur and V.V. Yanovskii, in: *Proc. Intern. Working Group on the Physics of Nonlinear Phenomena and Turbulence* (Naukova Dumka, Kiev, 1983) p. 1683 (in Russian); *Dokl. Akad. Nauk SSSR* 279 (1984) 96 [*Sov. Phys. – Dokl.* 29 (1984) 926].
- [33] R.Z. Sagdeev et al., in: *Nonlinear Phenomena in Plasma Physics and Hydrodynamics*, ed. R.Z. Sagdeev (Mir, Moscow, 1986) p. 137.
- [34] H. Effinger and S. Grossmann, *Z. Phys. B* 66 (1987) 289–304.
- [35] V.S. L'vov, preprint No. 53, Institute of Automation and Electrometry, Novosibirsk (1977).
- [36] E.A. Kuznetsov and V.S. L'vov, *Phys. Lett. A* 64 (1977) 157.
- [37] F.A. Kuznetsov and V.S. L'vov, *Physica D* 2 (1981) 203.
- [38] V.I. Belinicher and V.S. L'vov, *Zh. Eksp. Teor. Fiz.* 93 (1987) 533 [*Sov. Phys. – JETP* 66 (1987) 303].
- [39] P.C. Martin, E.D. Siggia and H.A. Roze, *Phys. Rev. A* 8 (1973) 423.
- [40] D. Foster, D.R. Nelson and M.J. Stephen, *Phys. Rev. A* 16 (1977) 732.
- [41] P.C. Martin and C. De Dominicis, *Prog. Theor. Phys. Suppl.* 64 (1978) 108.
- [42] S. Grossmann and E. Schnedler, *Z. Phys. B* 26 (1977) 307.
- [43] E. Levich, *Phys. Lett. A* 79 (1980) 171.
- [44] V. Yakhot, *Phys. Rev. A* 23 (1981) 1486.
- [45] C. De Dominicis and P.C. Martin, *Phys. Rev. A* 19 (1979) 419.
- [46] L.Ts. Adzhemyan, A.N. Vasil'ev and Yu.M. Pismak, *Teor. Mat. Fiz.* 57 (1983) 268 [*Theor. Math. Phys.* 57 (1983) 1131].
- [47] R.H. Kraichnan, *Phys. Rev. A* 25 (1982) 3281.
- [48] V. Yakhot and S.A. Orszag, *J. Sci. Comput.* 1 (1986) 3.
- [49] V. Yakhot and S.A. Orszag, *Phys. Rev. Lett.* 57 (1986) 1722.
- [50] W.P. Dannevik, V. Yakhot and S.A. Orszag, *Phys. Fluids* 30 (1987) 2021.
- [51] R.H. Kraichnan, *Phys. Fluids* 30 (1987) 2400.
- [52] E.V. Teodorovich, *Izv. Akad. Nauk SSSR Ser. Mekh. Zhidk. Gaza* No. 4 (1987) 29; *Prikl. Mat. Mekh.* 52 (1988) 218.
- [53] D. Ronis, *Phys. Rev. A* 36 (1987) 3322.
- [54] E.V. Teodorovich, *Zh. Eksp. Teor. Fiz.* 96 (1989) 163 [*Sov. Phys. – JETP* 69 (1989) 89].
- [55] A.A. Migdal, S.A. Orszag and V. Yakhot, *Intrinsic stirring force in turbulence and the ϵ -expansion*, preprint Princeton Univ. (1990).
- [56] E. Siggia, *J. Fluid Mech.* 107 (1981) 375.
- [57] Z.-S. She, E. Yackson and S.A. Orszag, in: *Proc. Newport Conf. on Turbulence* (Springer, Berlin, 1990).
- [58] D.I. Meiron, M.J. Shelley, W.T. Ashurst and S.A. Orszag, in: *Mathematical Aspects of Vortex Dynamics*, ed. R.E. Caflisch (Society for Industrial and Applied Mathematics, Philadelphia, 1989).
- [59] J.M. Kosterlitz and D.J. Thouless, *J. Phys. C* 6 (1979) 1181.
- [60] V.I. Belinicher and V.S. L'vov, *Scale-invariant theory of developed hydrodynamic turbulence*, preprint No. 385, Inst. Aut. Electrom., Novosibirsk (1987).
- [61] A. Lamb, *Hydromechanics* (Moscow, 1947).
- [62] V.E. Zakharov and V.S. L'vov, *Izv. VUZ. Radiofiz.* XVIII (1975) 1470.
- [63] V.E. Kuznetsov and A.V. Michailov, *Phys. Lett. A* 113 (1985) 266.
- [64] A.V. Tur and V.V. Yanovsky, preprint No. 1203, Space Research Institute, Moscow (1986).
- [65] V.F. Dmitriev, preprint No. 81–114, Institute of Nuclear Physics, Novosibirsk (1981).